

Differential equation and probability inspired graph neural networks for latent variable learning

Zhuangwei Shi*

Abstract—Probabilistic theory and differential equation are powerful tools for the interpretability and guidance of the design of machine learning models, especially for illuminating the mathematical motivation of learning latent variable from observation. State estimation and subspace learning are two classical problems in latent variable learning. State estimation solves optimal value for latent variable (i.e. state) from noised observation. Subspace learning maps high-dimensional features on low-dimensional subspace to capture efficient representation. Graphs are widely applied for modeling latent variable learning problems, and graph neural networks implement deep learning architectures on graphs. Inspired by probabilistic theory and differential equations, this paper proposes graph neural networks to solve state estimation and subspace learning problems. This paper conducts theoretical studies, and adopts empirical studies on several tasks, including text classification, protein classification, stock prediction and state estimation for robotics. Experiments illustrate that the proposed graph neural networks are superior to the current methods. Source code of this paper is available at <https://github.com/zshicode/Latent-variable-GNN>.

Index Terms—Subspace learning, differential equations, graph neural networks, state estimation, latent variable learning

CONTENTS

I	Introduction	2
II	Differential equation and probability inspired graph neural networks	3
II-A	ODE inspired graph neural networks . .	3
II-B	PDE inspired graph neural networks . .	3
II-B1	Heat conduction equation inspiration	3
II-B2	PDE inspired spectral GNN .	4
II-B3	PDE inspired spatial GNN .	4
II-C	On Laplacian matrix	5
II-D	Graph neural networks inspired by differential equation	6
II-D1	Label propagation and manifold learning	6
II-D2	Edge weight computation inspired by differential equation	6
III	Subspace learning guided graph neural networks	7
III-A	Low-rank sparsity and manifold	7
III-A1	Label propagation for subspace learning and semi-supervised learning on manifold	7

III-A2	Sparse and low-rank subspace	7
III-A3	Low-rank representation and label propagation	8
III-B	Numerical optimization methods for subspace learning	8
III-B1	Argumented Lagrangian multiplier	8
III-B2	Accelerated proximal gradient method	8
III-B3	Alternating Direction Method of Multipliers	9
III-C	Ridge regression and LASSO	9
III-D	Classifier based on variational graph autoencoder	9
III-D1	Learning from label propagation to GNN	9
III-D2	Variational graph autoencoder and subspace learning	9

IV State estimation via conditional random field based graph neural networks 10

IV-A	Kalman Filter and Kalman Smoother . .	10
IV-B	EM-KF algorithm	10
IV-C	Deep learning for sequential data	11
IV-D	Conditional random field based graph neural networks	12
IV-D1	Conditional random field and state estimation	12
IV-D2	Conditional random field in machine learning on graph .	12
IV-D3	Proposing GNN in CRF	13
IV-D4	Inductive learning	14
IV-D5	Modification of models for state estimation	14

V Experiments 14

V-A	Node classification for text classification	14
V-B	Graph classification for protein classification	15
V-C	State estimation for robotics	15
V-D	State estimation for stock prediction . .	16

VI Conclusions 17

Appendix A: Summary of subspace learning algorithms 17

Appendix B: Proof of theorems 18

Zhuangwei Shi is with the College of Artificial Intelligence, Nankai University, Tianjin 300350, China.

*Correspondence: zwshi@mail.nankai.edu.cn

Appendix C: Supplementary materials	21
C-A Label propagation parameter selection in POGNN	21
C-B Tentative networks that combine GCN and label propagation via subspace learning	22
C-C Indicators in stock prediction	22
References	23

I. INTRODUCTION

LATENT variable learning consists of algorithms that predict latent variable from observation. In control theory, latent variable is usually called *state*. State estimation is an important topic in automatic control and machine learning. State estimation is widely applied for robotics, computer vision, financial engineering, time-series forecasting and so on. As the state x and observation y in a system are usually disturbed by stochastic noise, state estimation aims to estimate the true state via observation. Optimal state estimation is to minimize the error between estimated states and true states.

Kalman Filter is the most classical method for state estimation, and is also considered as one of the most classical methods for latent variable learning. Kalman Filter provides a vivid instance how probabilistic theory and differential equation can inspire the design of machine learning models.

Kalman [26] proposed Kalman Filter (KF) to iteratively estimate state via observation in stochastic linear systems.

$$\begin{aligned}
 x_k &= Ax_{k-1} + w_k, \\
 y_k &= Cx_k + v_k, \\
 w_k &\sim N(0, Q), v_k \sim N(0, R), \\
 x_0 &\sim N(m_0, P_0), k = 1, 2, \dots, N,
 \end{aligned} \tag{1}$$

Here w, v denote white noise. There are some nonlinear extensions of Kalman Filter, such as Extended Kalman Filter (EKF), Unscented Kalman Filter (UKF, also known as sigma-point Kalman Filter) and Particle Filter (PF) [2].

However, there are two disadvantages of Kalman Filter that cannot be ignored.

- 1) KF requires model parameters. Although A, C are easy to obtain through system modeling, Q, R, m_0, P_0 depend on estimation by designers' experience.
- 2) Eq. (1) clarifies that KF assumes Markov property of states, and conditional independence of observations, yet actual systems do not follow these two assumptions usually.

To address the first issue, Expectation Maximization (EM) algorithm [12] was used for parameter estimation before filtering. Ghahramani and Hinton [17] proposed a method integrating Kalman Filter for state estimation and EM algorithm for parameter estimation in linear dynamic systems, and it is so called EM-KF algorithm. The EM-KF algorithm is also extended to nonlinear systems by combining EKF, UKF or PF.

To address the second issue, condition random field based approaches were proposed to state estimation for model long-term dependency. The Expectation Maximization (EM) algorithm and condition random field illustrate the broad way for

probabilistic graph model to inspire the research of differential equation and dynamic system. Neural networks are also used for model the complex dependency in latent variable learning.

The subspace learning problem is also defined from the motivation that predict latent variable from observation. The observed features X are usually high-dimensional, yet machine learning models perform much better on analyzing low-dimensional representations. The latent representations span the low-dimensional subspace. The subspace may follow some constraints, usually low-rank constraints, sparse constraints and manifold constraints. Such constraints can be modeled through numerical optimization programming, but usually with probabilistic theory and differential equation as well. Appendix summarizes some classical subspace learning methods.

Subspace learning usually conducts manifold constraint. Manifold constraint is motivated by the *manifold* in differential geometry, which can derive some remarkable partial differential equations (PDE). The Laplacian operator in PDE is correspond to the Laplacian matrix of a matrices. This idea can derive a series of ordinary differential equations (ODE) to describe the Laplacian-participated linear dynamic systems. Label propagation [54], [55], [65] follows manifold regularization [5]. For semi-supervised iterative algorithms such as label propagation algorithm and pagerank, establishing the equivalent relationship between its iterative equation and deep learning network can improve the effect of label propagation algorithm, and design semi-supervised iterative algorithms in deep learning network.

Graph neural networks [28], [42] (GNN) is widely applied to model graph relationship for deep learning [24], [25], [47]. Graphs are widely applied for modeling latent variable learning problems, and graph neural networks implement deep learning architectures on graphs.

Vanilla GNN focus on classification task upon nodes on a graph. The graph convolutional networks (GCN) [28], GraphSAGE [20], MPNN (message passing network) [18], graph attention networks (GAT) [53], graph autoencoders (GAE) [29], variational graph autoencoders (VGAE) [29], attention-based graph neural networks (AGNN) [50], graph isomorphism network (GIN) [59] and many other models were proposed. Subspace learning and differential equation guided graph neural networks [33], [56] are useful for detecting subspace with low-rank or sparse property, or with better manifold smoothness. Probabilistic theory inspired graph neural networks [29], [47], such as variational inference and conditional random field, are powerful for detecting latent variable dependency and learning efficient representation.

Graph neural networks do not only adopt on node classification, but also adopt on graph classification or graph pooling. This task focuses on representation learning from the whole graph. Basic methods were based on graph kernel [44]. Novel GNN for node classification, such as GCN [28] and GIN [59], can adopt for graph classification by adding mean pooling operator that outputs the mean vector of all feature vectors of nodes. However, researchers have proposed a series of graph neural network models mainly for graph pooling and graph classification tasks, such as Diffpool [62], EigenPool [36], graph u-net [16], and SAGPool [30].

In this paper, we propose differential equation and probability inspired graph neural networks for latent variable learning, focusing on subspace learning for node and graph classification, as well as state estimation.

- 1) We propose PDE and ODE inspired graph neural networks for node classification. It is so called POGNN.
- 2) We propose a variational graph autoencoder based subspace learning model for graph pooling and graph classification. It is so called VSPool.
- 3) We integrate Transformer and conditional random field based graph neural networks (CRF-GNN) for state estimation, and it is so called TCG-KF.

Numerical simulation on a linear mobile robot model, and empirical studies on stock prediction, demonstrate that the proposed method outperforms current methods. Part of the source code of this paper is available at <https://github.com/zshicode/Latent-variable-GNN>.

II. DIFFERENTIAL EQUATION AND PROBABILITY INSPIRED GRAPH NEURAL NETWORKS

A. ODE inspired graph neural networks

Deep learning and differential equations (dynamic systems) have certain equivalence under certain conditions. For example, ResNet can be regarded as the form of $x_{n+1} - x_n = f(x_n)$, which can be regarded as discretized $\dot{x} = f(x)$. For the optimal control form and feedback form of the differential (iterative) equation, the process of network training can be regarded as the process of solving the optimal control problem. Optimize the solution via Pontryagin's maximum principle (PMP) in optimal control [32], or design a new deep learning network e.g. NeuralODE [10], can improve the interpretability of the deep learning network.

When the graph neural network was first proposed, [42] was given in the form of an iterative equation, denoting the feature as X , the hidden state as H , and the output as O , then $H \leftarrow F(H, X)$, $O \leftarrow G(H^*, X)$. For the current general graph neural network, its message passing process can also be written in the form of an iterative equation. For example, the GCN in [28] can be written as (transductive learning)

$$\bar{\mathbf{h}}_i^{(k)} \leftarrow \frac{1}{d_i + 1} \mathbf{h}_i^{(k-1)} + \sum_{j=1}^n \frac{1}{\sqrt{(d_i + 1)(d_j + 1)}} \mathbf{h}_j^{(k-1)}, \quad (2)$$

GraphSAGE [20] can be written as (inductive learning)

$$\bar{\mathbf{h}}_i^{(k)} \leftarrow \frac{1}{d_i + 1} \left(\mathbf{h}_i^{(k-1)} + \sum_{j=1}^n \mathbf{h}_j^{(k-1)} \right), \quad (3)$$

PageRank [38] can be written as

$$h_u = \frac{1 - \alpha}{N} + \alpha \sum_{v \in \mathcal{N}(u)} \frac{h_v}{d_v} \quad (4)$$

Among them, α is called the damping factor, which is generally taken as 0.85, N is the number of nodes in the entire graph, and d represents the degree of the node, which is similar to the message passing mechanism of GCN.

Consider the one-dimensional Weisfeiler-Lehman (WL-1) algorithm

$$h_i^{(t+1)} \leftarrow \text{hash} \left(\sum_{j \in \mathcal{N}_i} h_j^{(t)} \right) \quad (5)$$

Here $h_i^{(t)}$ represents the "color" (i.e. label information) of the node v_i at the t th iteration, and \mathcal{N}_i represents its neighborhood. Replace the hash operation with a neural network, then

$$h_i^{(l+1)} = \sigma \left(\sum_{j \in \mathcal{N}_i} \frac{1}{c_{ij}} h_j^{(l)} W^{(l)} \right) \quad (6)$$

The discrete iteration is linked to dynamic programming. [60] considered graph neural networks with the relaxation step of Bellman-Ford algorithm.

$$d[t+1][i] = \min_{j \in \mathcal{N}_i} d[t][j] + w[j][i] \quad (7)$$

Inspired by the Neural ODE [10], [57] proposes a continuous graph neural network (continuous GNN), and uses the ordinary differential equation model to explain the GNN.

B. PDE inspired graph neural networks

1) *Heat conduction equation inspiration:* Use Δ to represent the Laplacian operator (harmonic operator), such as in the two-dimensional case

$$\Delta = \frac{\partial^2}{\partial x^2} + \frac{\partial^2}{\partial y^2} \quad (8)$$

Use Δ^2 for the biharmonic operator, e.g. in the two-dimensional case

$$\Delta^2 = \left(\frac{\partial^2}{\partial x^2} + \frac{\partial^2}{\partial y^2} \right)^2 = \frac{\partial^4}{\partial x^4} + 2 \frac{\partial^4}{\partial x^2 \partial y^2} + \frac{\partial^4}{\partial y^4} \quad (9)$$

On the graph Δ represents the normalized Laplacian matrix (the Laplacian operator on the discretized manifold), and the biharmonic operator $\Delta^2 \approx \Delta^T \Delta$

Theorem 1. *The following equality holds that*

$$\min y^T \Delta y \Leftrightarrow \min \|\nabla y\|^2 \quad (10)$$

Proof of all theorems are provided in Appendix.

Definition 1 (Heat conduction equation). *Heat u on manifold M*

$$\frac{\partial u}{\partial t} = \Delta u \quad (11)$$

Theorem 2. *Regard the label information as the temperature on the graph. When the "thermal equilibrium" is reached, that is, when the label propagation converges, there will be $\Delta u = 0$. Based on this, the edge weights of graph can be set as RBF (radius basis function) kernel [4], [37], [65].*

$$w_{ij} = \exp \left(-\frac{\|x_i - x_j\|^2}{4t} \right) \quad (12)$$

Laplacian eigenmap [4] defines edge weights according to (12) to solve optimization problems

$$\begin{aligned} \min \text{tr}(y^T L y) \\ \text{s.t. } y^T D y = 1, y^T D e = 0 \end{aligned} \quad (13)$$

where D, L represent the degree matrix and Laplacian matrix without regularization, and e is an all-one vector. Let $0 = \lambda_1 < \lambda_2 < \dots < \lambda_n$ be the eigenvalue of the generalized eigenvalue problem $Ly = \lambda Dy$, and take the $2 \sim m+1$ th element of each eigenvector to form m -dimensional features for each node.

Spectral clustering [37] is similar to [4], let $0 = \lambda_1 < \lambda_2 < \dots < \lambda_n$ be $D^{-1/2}LD^{-1/2}$, take the $2 \sim m+1$ element of each feature vector to form the m dimension feature of each node, and then perform k-means clustering. [45] proves that solving such an eigenvalue decomposition problem is equivalent to finding the optimal solution of a graph cut problem (i.e., normalized cut) (the sum of weights between classes is the smallest, and the sum of weights within classes is the largest).

$$\begin{aligned} \min Ncut &= \frac{y^T(D-W)y}{y^T Dy} \\ \text{s.t. } y^T De &= 0 \end{aligned} \quad (14)$$

This is applied to image segmentation. When the value of each element in the eigenvector corresponding to the second smallest eigenvalue is taken out, the image is thresholded according to this value (or k-means clustering is performed on each pixel. class) to get the result of image segmentation.

After [55] introduces hyperedge, the problem of solving the weight matrix can be written as the following optimization problem

$$\begin{aligned} \min_w \varepsilon &= \sum_i \|x_i - \sum_{j:x_j \in N(x_i)} w_{ij} x_j\|^2 \\ \text{s.t. } \sum_{j:x_j \in N(x_i)} w_{ij} &= 1, w_{ij} \geq 0 \end{aligned} \quad (15)$$

Proposition 1. First-order CRF is linked to $\min y^T \Delta y$, second order is linked to $y^T \Delta^2 y$. (See Theorem 18 and 19)

Now generalize (11) to the graph.

Definition 2 (Heat conduction equation on graph). For the heat u_i of node i we have

$$\Delta u_i = \sum_{j \in N(i)} w_{ij} u_j - d_i u_i \quad (16)$$

so

$$\Delta u = (W - D)u = -Lu \quad (17)$$

so

$$\partial u / \partial t = -Lu \quad (18)$$

Heat distribution $K_t = \exp(-tL)$, where $K_t(i, j)$ represents the heat conducted from i to j at time t . Kernel K_t is equivalent to setting edge weights as (12).

Theorem 3. [54] derived label propagation in such form

$$y_u^* = (I - W_{uu})^{-1} W_{ul} \bar{y}_l \quad (19)$$

via linear equation

$$(I - W_{uu} \quad -W_{ul}) \begin{pmatrix} (I - W_{uu})^{-1} W_{ul} \bar{y}_l \\ y_l \end{pmatrix} = 0 \quad (20)$$

Proposition 2. [66] suggests that the semi-supervised learning problem on the graph is equivalent to solving the harmonic

equation $\Delta y = 0$, and the boundary condition is the label of the marked point, which is equivalent to minimizing $y^T \Delta y$. The biharmonic operator is equivalent to minimizing $\|\Delta y\|^2$.

2) PDE inspired spectral GNN:

Proposition 3. Green function of (18)

$$G = \int_0^{+\infty} K_t dt = L^{-1} \quad (21)$$

After introducing Green function, y_u can be calculated like this

$$y_u = G_{uu} W_{ul} \bar{y}_l \quad (22)$$

which is

$$f(j) = \sum_{i=1}^l \sum_{k \in N(j)} y_i w_{ik} G(k, j) \quad (23)$$

This is how to write f as a kernel classifier.

Definition 3 (Heat kernel). The solution to the equation (18) is

$$K_t u(x, 0) = K_t f(x) = \int_M \kappa_t(x, y) f(y) dy \quad (24)$$

Where κ_t is called the heat kernel, and heat kernel has the following properties:

$$\kappa_t(x, y) = \sum_{i=1}^{+\infty} e^{-\lambda_i t} u_i^T(x) u_i(y) \quad (25)$$

where i is the i -th eigenvector of the Laplacian matrix.

In addition, the spectrum of $K_t = \exp(-tL)$ can also be studied, and if λ_i represents the eigenvalue of L , this group of basis $e^{-\lambda_i t}$ can be investigated. In the frequency domain, that is, a set of basis $e^{-j\omega t}$, which is the idea of *Fourier transform*. In fact, the Fourier transform is derived from the solution of the heat conduction equation.

Proposition 4. Note that the first-order Taylor expansion of $e^{-\lambda_i t}$ is $1 - \lambda_i t$, so it can be considered that $e^{-\lambda_i t} \approx (1 - \lambda_i t)^k$, while $(1 - \lambda_i)^k$ corresponds to the k order filter in the graph convolution.

Message passing process in the graph neural network can also be regarded as a process of "heat" propagation, and it can also be regarded as a kind of label propagation. (25) is very similar to the Fourier transform on a graph. And Fourier transform on the graph is closely related to the graph neural network.

3) PDE inspired spatial GNN: Above, we have proposed an understanding of the graph neural network method in the spectral domain.

For the graph neural network method in the spatial domain, for example, AGNN [50] calculates $e_{ij} = \beta \cos(z_i, z_j)$, Where $\beta \in (0, 1)$ is a learnable parameter, and then do softmax to get the weight

$$w_{ij} = \frac{\exp e_{ij}}{\sum_{k \in N(i)} \exp e_{ik}} \quad (26)$$

This is very similar to the RBF kernel because

$$\begin{aligned} e_{ij} &= -\frac{\|z_i - z_j\|^2}{2\sigma^2} \\ &= -\frac{2(1 - \cos(z_i, z_j))}{2\sigma^2} \\ &\stackrel{\text{def}}{=} -\beta(1 - \cos(z_i, z_j)), \\ &= \beta \cos(z_i, z_j) - \beta \end{aligned} \quad (27)$$

This is using the attention mechanism to learn edge weights similar to RBF.

C. On Laplacian matrix

The original Laplacian matrix

$$\mathcal{L} = D - A \quad (28)$$

In graph signal processing [56], graph filtering problems often correspond to the following optimization problems

$$\min_x x^T \mathcal{L}x \quad \text{s.t. } x^T D x = \text{trace} D \quad (29)$$

in

$$x^T \mathcal{L}x = \frac{1}{2} \sum_{i,j} a_{ij} (x_i - x_j)^2 \quad (30)$$

is called the total variation operator, the Lagrange multiplier of the above optimization problem is

$$x^T \mathcal{L}x - \lambda(x^T D x - \text{trace} D) \quad (31)$$

So the solution is the generalized eigenvalue problem as follows

$$\mathcal{L}x = \lambda D x \Leftrightarrow D^{-1} \mathcal{L}x = \lambda x \quad (32)$$

Its generalized Rayleigh entropy is

$$R = \frac{x^T \mathcal{L}x}{x^T D x} \quad (33)$$

Let $y = D^{1/2}x$ then

$$R = \frac{y^T D^{-1/2} \mathcal{L} D^{-1/2} y}{y^T y} \quad (34)$$

This leads to two forms of regularized Laplacian matrix, one of which is the symmetric regularized Laplacian matrix

$$L = D^{-1/2} \mathcal{L} D^{-1/2} = I - D^{-1/2} A D^{-1/2} \quad (35)$$

The second is the regularized Laplacian matrix of the random walk

$$L_{rw} = D^{-1} \mathcal{L} = I - D^{-1} A \quad (36)$$

Note that $D^{-1}A$ is exactly the state transition matrix of the random walk (this Markov process).

$D^{-1}A$ is similar to $D^{-1/2} A D^{-1/2}$ and has the same eigenvalues, if v is $D^{-1}A$, then $D^{1/2}v$ is the eigenvector of the eigenvalue corresponding to $D^{-1/2} A D^{-1/2}$.

Theorem 4 (Spectral radius of non-negative matrix). *For a non-negative matrix A of order n :*

$$\min_i \sum_j a_{ij} \leq \rho(A) \leq \max_i \sum_j a_{ij} \quad (37)$$

$$\min_j \sum_i a_{ij} \leq \rho(A) \leq \max_j \sum_i a_{ij} \quad (38)$$

Theorem 5 (Perron-Frobenius). *If A is a non-negative matrix of order n , then:*

- $\rho(A) > 0$, and the algebraic multiplicity of the eigenvalue corresponding to $\rho(A)$ is 1;
- There is a unique vector x such that $Ax = \rho(A)x$, and $x_i > 0$, $\sum_i x_i = 1$, called the right Perron vector;
- There is a unique vector y such that $y^T A = \rho(A)y^T$, and $y_i > 0$, $\sum_i x_i y_i = 1$, called the left Perron vector;
- If A is a positive matrix, then the geometric multiplicity of the eigenvalue corresponding to $\rho(A)$ is 1, and

$$\lim_{m \rightarrow \infty} (\rho(A)^{-1} A)^m = xy^T \quad (39)$$

Theorem 6 (Eigenvalues of the regularized Laplacian matrix). *The eigenvalues of the regularized Laplacian matrix lie in the interval $[0, 2]$, and for any graph (the number of nodes is not less than 2), L has an eigenvalue of 0, only for bipartite graphs, L has an eigenvalue of 2.*

[33] used the above properties to explain the over-fitting problem of GCN, and proposed a method for co-training and self-training of GCN to avoid over-fitting. Regardless of the activation function, the one-step iteration formula of GCN is $H = \hat{A}X\Theta$, so multi-layer GCN can be written as

$$Z = \hat{A} \cdots \hat{A} X \Theta_1 \cdots \Theta_k = \hat{A}^k X \Theta_1 \cdots \Theta_k \quad (40)$$

Let $\hat{A} = D^{-1}A$, since $\rho(\hat{A}) = 1$, so

$$\lim_{k \rightarrow \infty} \hat{A}^k = \begin{pmatrix} 1/\sqrt{n} \\ \vdots \\ 1/\sqrt{n} \end{pmatrix} \cdot 1 \cdot (1/\sqrt{n}, \dots, 1/\sqrt{n}) = \frac{1}{n} E \quad (41)$$

where e represents an all-one matrix. This means that in a deep GCN, if no improvement is made, the features are equivalent to propagating on a (including self-loop) fully connected graph. After neighborhood aggregation, the features at all points converge, making the GCN classification Ability is significantly reduced.

Proposition 5. *The optimal number of layers k of GCN satisfies*

$$\bar{d}^k n_l = n \quad (42)$$

Where \bar{d} represents the average degree of nodes, n_l, n represent the number of marked nodes and the total number of nodes, respectively. This means that after k layers of GCN, the features on the marked nodes can just be transferred to the full graph. [33]

The following considers adding a self-loop to the graph, $\tilde{A} = A + \gamma I$, (generally $\gamma = 1$), [56]. These discussions are for undirected unweighted graphs (i.e., the adjacency matrix is symmetric 0-1 matrix).

Proposition 6. *Adding a self-loop to the graph can reduce the maximum eigenvalue of the regularized Laplacian matrix.*

Theorem 7. *conjecture that the*

$$\tilde{\lambda}_n = 1 - \frac{\gamma}{\gamma + \bar{d}} - \frac{\bar{d}}{\gamma + \bar{d}} \beta_1 \quad (43)$$

As an estimate of $\tilde{\lambda}_n$, $-1 < \beta_1 < 0$ and generally $\beta_1 \approx -1$, so

$$\tilde{\lambda}_n \approx 1 - \frac{\gamma}{\gamma + \bar{d}} + \frac{\bar{d}}{\gamma + \bar{d}} = \frac{2\bar{d}}{\gamma + \bar{d}} \quad (44)$$

This approximation can significantly reduce the amount of computation for $\tilde{\lambda}_n$, in fact, \bar{d} is the quotient of the total number of edges divided by the total number of nodes, in other words, the sum of adjacency matrix elements divided by the matrix order's business.

D. Graph neural networks inspired by differential equation

1) *Label propagation and manifold learning*: A graph is the discretized form of a manifold, thus f can also be regarded as the discretized form of f , with its values equivalent to the values of f at the nodes of the graph. In such a viewpoint, the matrix $I - W$ can be regarded as the graph Laplacian of this pasted graph intuitively. L is the Laplacian-Beltrami operator defined on the data manifold, and f is the function defined on this manifold.

Proposition 7. *Semi-supervised learning problem on the graph is equivalent to solving the harmonic equation $\Delta f = 0$, and the boundary condition is the label of the marked point, which is equivalent to minimizing $f^T \Delta f$. Minimizing $f^T \Delta f$ is equivalent to minimizing $\|\nabla f\|^2$.*

Proposition 8. *Use L to represent the regularized Laplacian matrix, in the spectral clustering [37], convert the solution equation $Lf = 0$ (that is, find the eigenvector of L) to minimize $f^T Lf$, and solving such an eigenvalue decomposition problem is equivalent to finding an optimal solution to a graph cut problem (i.e., normalized cut).*

Proposition 9. *Relax the solution equation $Lf = 0$ (that is, find the eigenvector of L) to minimize $\|Lf\|^2 = f^T L^T Lf$, that is, solve the equation $L^T Lf = 0$, that is, the biharmonic equation $\Delta^2 f = 0$.*

Label propagation can be regarded as a Laplacian least square method [5], and its optimization objective is

$$\min_F F^T L F + \frac{\gamma}{2} \|F - Y\|_F^2 \quad (45)$$

Considering that the regularized Laplace matrix can be written as $L = I - W$, where W is the normalized edge weight, the optimal solution is $F^* = (1 - \alpha)(I - \alpha W)^{-1}Y$, here $\alpha = 1/(1 + \gamma)$. This can be obtained by iterating $F^{(k)} = \alpha W F^{(k-1)} + (1 - \alpha)Y$, $0 < (1 - \alpha) \ll 1$. Let $\eta = 2/\gamma$,

$$\begin{aligned} & \min_F \eta \text{tr}(F^T L F) + \|Y F\|^2 \\ & \Rightarrow \eta L F + Y F = 0 \\ & \Rightarrow F = (I + \eta L)^{-1} Y \end{aligned}$$

And when the spectral radius of ηL is not greater than 1, the first-order Taylor expansions of $(I + \eta L)^{-1}$ and $e^{-\eta L}$ are both

$I - \eta L$. Use $F = W(W + \eta L)^{-1}Y$ to find F [58], where η is a hyperparameter, then

$$\begin{aligned} F &= W(W + \eta L)^{-1}Y \\ &= W(W^{-1} - W^{-1}(\eta L)(I + \eta L)^{-1})Y \\ &= (I - \eta L(I + \eta L)^{-1})Y \\ &= (I + \eta L)^{-1}Y \end{aligned}$$

In this paper, when using GCN for node classification, the iterative form of GCN is

$$H_{k+1} = (I + \eta L)^{-1} H_k \Theta_k, \eta > 1 \quad (46)$$

It is propagated according to the label. The formula $F = (I + \eta L)^{-1}Y$ improves the practice of GCN. This paper sets $\eta = 2$. The label propagation parameter η selection in POGNN is on Appendix.

Theorem 8. *The graph filtering that combines graph convolution and label propagation [33], suggests that label propagation algorithm is an optimization problem*

$$\min_Z \|Z - Y\|^2 + \alpha \text{trace}(Z^T L Z) \quad (47)$$

so

$$Z = (I + \alpha L)^{-1} Y \quad (48)$$

where L is the (normalized) Laplacian matrix and Y is the label.

Remark of this Theorem is on Appendix.

2) *Edge weight computation inspired by differential equation*: The label propagation algorithm is similar in form to the graph neural network. The edge weight of the label propagation algorithm is determined according to the distance between the features. The goal is to make the weight between the similar feature points as large as possible. In the graph neural network, the weight of the edge is set according to the actual problem, or learn it with the attention mechanism. e.g. [53] setting

$$\begin{aligned} z_i^{(l)} &= \Theta^{(l)} h_i^{(l)} \\ e_{ij}^{(l)} &= \text{LeakyReLU}(\bar{a}^{(l)T} (z_i^{(l)} \| z_j^{(l)})) \\ w_{ij}^{(l)} &= \frac{\exp(e_{ij}^{(l)})}{\sum_{k \in \mathcal{N}(i)} \exp(e_{ik}^{(l)})} \\ h_i^{(l+1)} &= \sigma \left(\sum_{j \in \mathcal{N}(i)} w_{ij}^{(l)} z_j^{(l)} \right) \end{aligned} \quad (49)$$

Where Θ, a is the parameter learned by the neural network. AGNN [50] uses the process of calculating the above e_{ij} to be replaced by cosine similarity, $e_{ij} = \beta \cos(z_i, z_j)$, where $\beta \in (0, 1)$ is a learnable parameter. MPNN (message passing network) [18] uses a fully connected layer to map the feature vector of the source node to the edge weight, ie $w_{ij} = F F N N(z_j)$.

Edge weight computation

- RBF kernel form computation inspired by PDE

Node classification

- Label propagation inspired by manifold learning and ODE

Fig. 1. POGNN

Calculate w_{ij} using RBF

$$\begin{aligned} e_{ij} &= -\frac{\|z_i - z_j\|^2}{2\sigma^2} \\ &= -\frac{2(1 - \cos(z_i, z_j))}{2\sigma^2} \\ &\stackrel{\text{def}}{=} -\beta(1 - \cos(z_i, z_j)), \\ w_{ij} &= \frac{\exp e_{ij}}{\sum_{k \in \mathcal{N}(i)} \exp e_{ik}} \end{aligned} \quad (50)$$

where $\beta \in (0, 1)$ is a learnable parameter.

The proposed PDE and ODE inspired graph neural networks is shown on Fig. 1. It is so called POGNN. The iteration procedure $H_{k+1} = (I + \eta L)^{-1} H_k \Theta_k$ is inspired by ODE theory on label propagation, as well as manifold learning motivated by PDE. The RBF and neural network based edge weights computation is also inspired by PDE and ODE.

III. SUBSPACE LEARNING GUIDED GRAPH NEURAL NETWORKS

A. Low-rank sparsity and manifold

1) *Label propagation for subspace learning and semi-supervised learning on manifold:* When there are few labeled samples, some assumptions must be made that relate the data distribution information revealed by the unlabeled samples to the class labels. The essence of the assumption is that "similar samples have similar outputs".

Definition 4 (Manifold assumption). *Assuming that the data is distributed on a manifold, points on the same structure are more likely to have the same label value.*

Definition 5 (Smoothness assumption). *Assuming that two closely samples in a dense region have similar labels, otherwise, when they are separated by sparse data regions, their labels tend to be different.*

Definition 6 (Cluster assumption). *Assuming that the data has a cluster structure, samples in the same cluster belong to the same category, that is, points with similar distances have the same label.*

The first and second assumptions consider the local consistency of points, and the third assumption considers the global consistency of points. These three assumptions stand for *semi-supervised learning*, and suggest that the data is distributed on subspace spanned through features.

Semi-supervised learning can be divided into two categories:

- **Transductive learning:** There is an intersection between unlabeled data and test samples, and the features of unlabeled data can be used for model training. The purpose of training is to give the optimal label to the unlabeled data in the current dataset.
- **Inductive learning:** There is no intersection between unlabeled data and test samples, the features of unlabeled data are not used for model training, and the purpose of training makes it applicable The learner on unlabeled data has the best generalization performance.

[66] first proposed a method for semi-supervised learning by using label information to propagate on the graph, and then proposed a method based on Gaussian random fields and harmonic functions (i.e. Laplacian operator/Laplacian matrix). On this basis, [65] proposed a label propagation algorithm as described below. The label propagation algorithm is a semi-supervised and transductive learning method.

The label propagation algorithm can be regarded as the idea of

- graph-based unsupervised learning
- manifold learning
- representation learning
- subspace learning
- semi-supervised learning

methods, including Laplacian feature map (Laplacian Eigenmap, LE) [4], Spectral clustering (Spectral clustering) [37], manifold regularization [5] are introduced into the problem of semi-supervised classification. In this methods, graph structure depicts subspace. Graph structure is learned through node features.

2) *Sparse and low-rank subspace:* [15] first proposed a method for clustering on sparse subspaces to solve the problem

$$\begin{aligned} \min_Z \|Z\|_0 \\ \text{s.t. } X = XZ \end{aligned} \quad (51)$$

The problem is NP-hard, so the convex relaxation is

$$\begin{aligned} \min_Z \|Z\|_1 \\ \text{s.t. } X = XZ \end{aligned} \quad (52)$$

Liu et al. proposed [35] that sparse representation does not consider the global constraints of data, while low rank can reflect the global relationship of data, and when hidden data is added, low rank represents data that can still be effectively learned features.

$$\begin{aligned} \min_Z \text{rank}(Z) \\ \text{s.t. } X = AZ \end{aligned} \quad (53)$$

The problem is NP-hard, so a convex relaxation is performed and a noise term E is added to give

$$\begin{aligned} \min_{Z, E} \|Z\|_* + \lambda \|E\|_{2,1} \\ \text{s.t. } X = XZ + E \end{aligned} \quad (54)$$

Where $\|\cdot\|_*$ represents the nuclear norm, that is, the sum of the singular values of the matrix, $\|E\|_{2,1} = \sum_j \sqrt{\sum_i e_{ij}^2}$ represents the $\ell_{2,1}$ norm, $\lambda > 0$.

High-dimensional features can be characterized by low-rank subspaces. Clustering high-dimensional data can be regarded as dividing it into different subspaces (subspace segmentation). Learning low-rank representation Z from high-dimensional data X , instead of directly constructing adjacency matrix W by X in NCut [45] and spectral clustering [37], the final $W = (|Z^*| + |Z^{*T}|)/2$.

NCut, spectral clustering, and low-rank representation are methods for constructing the topology of graphs entirely through features, while DeepWalk [39] is a method for learning node features on graphs entirely through topology. GCN [28] is a learning method that combines topology and feature matrix.

3) *Low-rank representation and label propagation*: In order to better derive the weight W required for label propagation through Z , [67] adds constraints to solve the following optimization problem

$$\begin{aligned} \min_{Z,E} \|Z\|_* + \lambda \|E\|_{2,1} \\ \text{s.t. } X = XZ + E, Z^T e = e, Z_{ij} = 0, \forall i, j \in \Omega \end{aligned} \quad (55)$$

Where e is a vector of all 1s, Ω is a set of edges, when x_i, x_j are marked and are not in the same class, this constraint can be expressed as a projection operator P_Ω , such that $P_\Omega(Z) = 0$. In this way, the optimization problem can be written as in ADMM. remember

$$A(Z) = \begin{pmatrix} \text{vec}(XZ) \\ Z^T e \\ P_\Omega(Z) \end{pmatrix}, B(E) = \begin{pmatrix} \text{vec}(E) \\ 0 \\ 0 \end{pmatrix}, c = \begin{pmatrix} \text{vec}(X) \\ 1 \\ 0 \end{pmatrix} \quad (56)$$

The vec operator means that the columns of the matrix are connected end to end and spliced into a longer column vector, then

$$\begin{aligned} \min_{Z,E} \|Z\|_* + \lambda \|E\|_{2,1} \\ \text{s.t. } A(Z) + B(E) = c \end{aligned} \quad (57)$$

B. Numerical optimization methods for subspace learning

1) *Argumented Lagrangian multiplier*: In [35], the augmented Lagrange multiplier method is used to solve the low-rank representation. And [34] is an improved Alternating Direction Method of Multipliers [7], that is, Linear Alternating Direction Method with Adaptive Penalty (LADMAP), to find low rank representation Methods.

[35] transforms the optimization problem (54) into

$$\begin{aligned} \min_{Z,E} \|J\|_* + \lambda \|E\|_{2,1} \\ \text{s.t. } X = XZ + E, Z = J \end{aligned} \quad (58)$$

The above optimization problem is solved using the augmented Lagrangian multiplier (ALM) method. The augmented Lagrangian function adds an F-norm term to the original Lagrangian function.

$$\begin{aligned} \min_{Z,E,J,Y_1,Y_2} \|J\|_* + \lambda \|E\|_{2,1} + \\ \text{tr}[Y_1^t(X - XZ - E)] + \text{tr}[Y_2^t(Z - J)] + \\ \frac{\mu}{2} (\|X - XZ - E\|_F^2 + \|Z - J\|_F^2) \end{aligned} \quad (59)$$

Theorem 9 (Singular Value Threshold). *Optimization [8]*

$$\min_X \lambda \|X\|_* + \frac{1}{2} \|X - A\|_F^2 \quad (60)$$

The solution is the SVT operator

$$S_\lambda(A) = U \text{diag}(\max(0, s_i - \lambda)) V^T \quad (61)$$

where USV^T is the singular value decomposition of A .

Theorem 10. *Optimization [35]*

$$\min_W \lambda \|W\|_{2,1} + \frac{1}{2} \|W - Q\|_F^2 \quad (62)$$

For the i column, it corresponds to the following proximal operator optimization problem

$$\min_{w_i} \lambda \|w_i\|_1 + \frac{1}{2} \|w_i - q_i\|_2^2 \quad (63)$$

It is solved as

$$S_\lambda(w_i) = \begin{cases} \frac{\|q_i\| - \lambda}{\|q_i\|} q_i & \lambda < \|q_i\| \\ 0 & \text{otherwise} \end{cases} \quad (64)$$

The S_λ in the above theorem is often called the shrinkage operator or the soft thresholding function.

2) *Accelerated proximal gradient method*: [34] gives the solution using accelerated proximal gradient (APG) [51] and proximal alternating direction method (i.e. ADMM with proximal operator) (54) process.

Consider the optimization problem $\min_X F(X) = P(X) + f(X)$. Do Taylor expansion of $F(X)$ at Y

$$\begin{aligned} Q_\tau(X, Y) &:= f(Y) + \langle \nabla f(Y), X - Y \rangle + \frac{\tau}{2} \|X - Y\|_F^2 + P(X) \\ &= \frac{\tau}{2} \|X - G\|_F^2 + P(X) + f(Y) - \frac{1}{2\tau} \|\nabla f(Y)\|_F^2 \end{aligned} \quad (65)$$

in

$$G = Y - \tau^{-1} \nabla f(Y) \quad (66)$$

but

$$\min_X F(X) = \min_X P(X) + \frac{\tau}{2} \|X - G\|_F^2 \quad (67)$$

Here P can be the nuclear norm, $\ell_{2,1}$ norm, etc. When $f(X) = \|AX - B\|_F^2/2$, $\nabla f(X) = AX - B$. The method of converting $\min_X F(X) = P(X) + f(X)$ into an optimization problem of the form (67) is called the proximal gradient method.

We use the speedup Nesterov trick, which is to set

$$Y_k = X_k + \frac{t_{k-1} - 1}{t_k} (X_k - X_{k-1}) \quad (68)$$

Theorem 11. *In the above algorithm, when $t_k = 1, \forall k$, the algorithm degenerates into the ordinary proximal gradient method, after iterating k times*

$$\exists L_f > 0, F(X_k) - F(X^*) \leq \frac{L_f \|X_0 - X^*\|_F^2}{2k} \quad (69)$$

That is to say, its convergence rate is $O(1/k)$, where the Lipschitz constant $L_f = \tau_k$. In other words, after $O(L_f/\varepsilon)$ iterations, $|F(X_k) - F(X^*)|$ converges to the order of ε , so sometimes the convergence rate is also recorded as $O(1/\varepsilon)$ [51].

Theorem 12. In the above algorithm, when $t_k \geq (k+2)/2$, the algorithm convergence rate is $O(1/\sqrt{\varepsilon})$, that is, the convergence rate after iteration k is $O(1/k^2)$ [51].

Theorem 13. In the above algorithm, when $t_{k+1}^2 - t_k \leq t_k^2$, the algorithm convergence rate is $O(1/\sqrt{\varepsilon})$, the above formula takes The equal sign gets $t_{k+1} = (1 + \sqrt{4t_k^2 + 1})/2$ [51].

3) *Alternating Direction Method of Multipliers*: Alternating Direction Method of Multipliers (ADMM) [7] Solve as

$$\begin{aligned} \min_{x,z} & f(x) + g(z) \\ \text{s.t.} & Ax + Bz = c \end{aligned} \quad (70)$$

The optimization problem of augmented Lagrange multipliers

$$L_\rho(x, z, y) = f(x) + g(z) + y^T(h(x, z)) + (\rho/2)\|h(x, z)\|_2^2 \quad (71)$$

$$h(x, z) = Ax + Bz - c \quad (72)$$

The iterative steps are

$$\begin{aligned} x^{k+1} &:= \operatorname{argmin}_x L_\rho(x, z^k, y^k) \\ z^{k+1} &:= \operatorname{argmin}_z L_\rho(x^{k+1}, z, y^k) \\ y^{k+1} &:= y^k + \rho(Ax^{k+1} + Bz^{k+1} - c) \end{aligned} \quad (73)$$

Remember the residual $r = Ax + Bz - c$, then

$$\begin{aligned} y^T r + (\rho/2)\|r\|_2^2 &= (\rho/2)\|r\|_2^2 + (1/\rho)y\|_2^2 - (1/2\rho)\|y\|_2^2 \\ &= (\rho/2)\|r + u\|_2^2 - (\rho/2)\|u\|_2^2 \end{aligned} \quad (74)$$

So there is the scaled form of ADMM

$$\begin{aligned} x^{k+1} &:= \operatorname{argmin}_x (f(x) + (\rho/2)\|Ax + Bz^k - c + u^k\|_2^2) \\ z^{k+1} &:= \operatorname{argmin}_z (g(z) + (\rho/2)\|Ax^{k+1} + Bz - c + u^k\|_2^2) \\ u^{k+1} &:= u^k + Ax^{k+1} + Bz^{k+1} - c \end{aligned} \quad (75)$$

where $u = y/\rho$.

Theorem 14 (ADMM convergence rate). *ADMM converges under certain conditions (generally satisfied), its convergence rate is similar to that of ALM, which is $O(1/k)$.*

In practical operation, the convergence rate of ADMM is significantly slower than that of gradient descent, Newton's method, etc. The main application of ADMM is when the size of the solution space is very large, such as a matrix of GB in storage space. At this time, many traditional methods are not easy to use, and it is forced to solve in blocks, and the absolute accuracy of the solution is often not so high. Also note:

- 1) ADMM generalized from 2-block to multi-block is not necessarily convergent.
- 2) In ADMM, when the value of ρ decreases with iteration, such as [34], it often works better, but it is also more difficult to analyze.

C. Ridge regression and LASSO

Definition 7 (Tikhonov regularization, ℓ_2 regularization). *Linear Least Squares Problem with Regularization of ℓ_2 Norm*

$$\min_x \|Ax - b\|_2^2 + \lambda \|Lx\|_2^2 \quad (76)$$

closed-form solution

$$x^* = (A^T A + L^T L)^{-1} A^T b \quad (77)$$

Compared with the ℓ_2 regularization, the ℓ_1 regularization is less sensitive to outliers, and the obtained solution is more sparse. For example, in robust PCA [9], it is the optimization

$$\begin{aligned} \min_{L,S} & \|L\|_* + \rho \|S\|_1 \\ \text{s.t.} & M = L + S \end{aligned} \quad (78)$$

ℓ_2 regularization and ℓ_1 regularization are often referred to as ridge regression and LASSO (Least Absolute Shrinkage and Selection Operator), respectively.

The solution of LASSO can be obtained by the proximal gradient method, which is called iterative shrinkage thresholding algorithm (ISTA) [11].

Theorem 15 (ISTA). *Linear Least Squares Problem with Regularization of ℓ_1 Norm*

$$\min_x \|Ax - b\|_2^2 + \lambda \|x\|_1 \quad (79)$$

solution

$$x_{k+1} = S_{\lambda/t}(x_k - \frac{1}{t} A^T (Ax_k - b)) \quad (80)$$

in

$$S_\lambda(x) = \begin{cases} 0 & |x| \leq \lambda \\ x - \lambda \cdot \operatorname{sign}(x) & |x| > \lambda \end{cases} \quad (81)$$

Theorem 16 (FISTA). *The accelerated proximal gradient method is used in ISTA to obtain FISTA (fast iterative shrinkage thresholding algorithm) [3], and the convergence speed is increased from $O(1/\varepsilon)$ to $O(1/\sqrt{\varepsilon})$.*

D. Classifier based on variational graph autoencoder

1) *Learning from label propagation to GNN*: Both label propagation algorithms and graph neural networks can be widely used in weakly supervised problems. The convergence of the label propagation algorithm is derived from the Perron-Frobenius theorem, and [42] proves the convergence of graph neural networks, which can be guaranteed by Banach's fixed point theorem.

The label propagation algorithm can only detect the subspace well when the node feature dimension is low, while the graph neural network is better at capturing information from high-dimensional, sparse features. It can be explored to use the graph neural network to first roughly estimate the subspace for dimensionality reduction before label propagation.

2) *Variational graph autoencoder and subspace learning*: Variational graph autoencoder (VGAE) [29] is a method of adding GCN to the encoding-decoding structure and variational inference to learn the low-dimensional and low-rank representation of node features on the graph [47]. We can first use the high-dimensional feature X to roughly estimate an adjacency matrix W_0 , then input W_0 and X into VGAE, learn the low-dimensional representation μ , and calculate it by μ New W for the label propagation process. Based this idea, this paper designs three tentative networks that combine GCN and label propagation via subspace learning for node classification on Cora. The procedure is on Appendix.

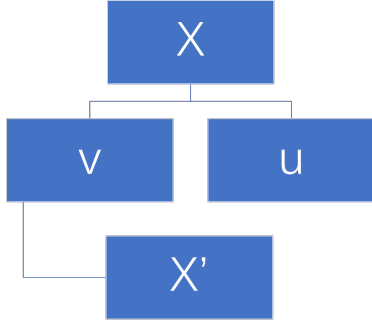


Fig. 2. VSPool

This paper proposes a VGAE based subspace learning model for graph classification as Fig. 2, named VSPool. It uses a variational graph autoencoder to map the features of nodes $X \in \mathbb{R}^{n \times m}$ to subspace vector $v_{n \times 1}$, and then adopt v to reconstruct features $X' \in \mathbb{R}^{n \times m}$. Note that

$$u = X^T v \in \mathbb{R}^{n \times m}, \forall n. \quad (82)$$

Output u can be the representation of a graph. The loss function is the sum of reconstruction error, classification error and Kullback-Leibler divergence.

Proximal operator is adopted to provide the sparsity of v .

$$v \leftarrow S_\lambda(v) = \begin{cases} 0 & |v_i| \leq \lambda \\ v_i - \lambda \cdot \text{sign}(v_i) & |v_i| > \lambda \end{cases} \quad (83)$$

where λ is the mean value of v .

IV. STATE ESTIMATION VIA CONDITIONAL RANDOM FIELD BASED GRAPH NEURAL NETWORKS

A. Kalman Filter and Kalman Smoother

Let $y_{1:k}$ denotes the observation of a system at $1 \sim k$, when $y_{1:k}$ and parameters of Eq. (1), A, C, Q, R, m_0, P_0 , have already been known, Kalman Filter recursively and forwardly estimates x_k from x_{k-1} .

$$p(x_k|y_{1:k}) = N(x_k|m_{k|k}, P_{k|k}). \quad (84)$$

Here, $N(x|m, P)$ denotes that x follows a Gaussian distribution, whose mean value is m and covariance matrix is P . Kalman Filter is an online state estimation algorithm, when $y_{1:N}$ (i.e. observation of the whole process), along with model parameters, have already been known, state estimation can be obtained via offline way, which is more precise. This is Kalman Smoother (KS) [41], also known as Rauch-Tung-Striebel Smoother or RTS Smoother. Based on the computation of Kalman Filter, Kalman Smoother estimates the state recursively and forwardly, for each $k = N-1, N-2, \dots, 0$.

$$p(\hat{x}_k|y_{1:N}) = N(\hat{x}_k|m_{k|N}, P_{k|N}), \quad (85)$$

The state estimation obtained through Kalman Filter or Kalman Smoother, is least square estimation (LSE) from control and optimization perspective, along with maximum likelihood estimation (MLE) and maximum a posteriori estimation (MAP) from statistics and probability perspective [2].

Kalman Filter recursively obtains the optimal estimation of x_k through the following steps.

- 1) Initialization. $m_{0|0} = m_0, P_{0|0} = P_0$.
- 2) For $k = 1, 2, \dots, N$, from the estimation at moment $k-1$, when the state is with mean value $m_{k-1|k-1}$ and variance $P_{k-1|k-1}$, to compute the one-step prediction from $k-1$ to k .

$$p(x_k|y_{1:k-1}) = N(x_k|m_{k|k-1}, P_{k|k-1}), \quad (86)$$

where mean value and variance are

$$m_{k|k-1} = A m_{k-1|k-1}, \quad (87)$$

$$P_{k|k-1} = A P_{k-1|k-1} A^T + Q, \quad (88)$$

respectively.

- 3) The optimal state estimation of $m_{k|k}$, is the linear combination of $m_{k|k-1}$, along with residual $r_k = y_k - C m_{k|k-1}$ (also known as innovation).

$$m_{k|k} = m_{k|k-1} + H_k(y_k - C m_{k|k-1}), \quad (89)$$

where H_k is Kalman Filter gain.

- 4) When deriving least square estimation, H_k can be obtained through solving equation $\frac{\partial \text{tr} P_{k|k}}{\partial H_k} = 0$, then $P_{k|k}$ can be obtained as well. When deriving maximum a posteriori estimation and maximum likelihood estimation, H_k and $P_{k|k}$ can be obtained through Bayes theorem.

$$H_k = P_{k|k-1} C^T (C P_{k|k-1} C^T + R)^{-1}, \quad (90)$$

$$P_{k|k} = (I - H_k C) P_{k|k-1}. \quad (91)$$

- 5) Finally, $m_{k|k}$ is the optimal filtering estimation of x_k .

$$p(x_k|y_{1:k}) = N(x_k|m_{k|k}, P_{k|k}). \quad (92)$$

Similarly, in Kalman Smoother

$$p(\hat{x}_k|y_{1:N}) = N(\hat{x}_k|m_{k|N}, P_{k|N}), \quad (93)$$

where

$$m_{k|N} = m_{k|k} + J_k(m_{k+1|N} - m_{k+1|k}), \quad (94)$$

$$P_{k|N} = P_{k|k} + J_k(P_{k+1|N} - P_{k+1|k}) J_k^T. \quad (95)$$

Kalman smoother gain

$$J_k = P_{k|k} A^T P_{k+1|k}^{-1}. \quad (96)$$

In a word, for $k = N-1, N-2, \dots, 0$, Kalman Smoother iterates optimal state estimation at the opposite direction of Kalman Filter.

B. EM-KF algorithm

Expectation Maximization (EM) algorithm iteratively computes the maximum likelihood estimation (MLE) of parameters when the probability distribution function (PDF) is with latent variables. According to Jensen's inequality,

$$\begin{aligned} \log p(y_{1:N}|\theta) &= \log \left(\int q(x_{0:N}) \frac{p(x_{0:N}, y_{1:N}|\theta)}{q(x_{0:N})} dx_{0:N} \right) \\ &\geq \int q(x_{0:N}) \log \frac{p(x_{0:N}, y_{1:N}|\theta)}{q(x_{0:N})} dx_{0:N}. \end{aligned} \quad (97)$$

Let $\theta^{(n)}$ denotes the parameters at n -th iteration, the PDF of latent variables

$$q(\mathbf{x}_{0:N}) := p(\mathbf{x}_{0:N} | \mathbf{y}_{1:N}, \theta^{(n)}), \quad (98)$$

Substitute Eq. (98) into Eq. (97),

$$\begin{aligned} & \int p(\mathbf{x}_{0:N} | \mathbf{y}_{1:N}, \theta^{(n)}) \log \frac{p(\mathbf{x}_{0:N}, \mathbf{y}_{1:N} | \theta)}{p(\mathbf{x}_{0:N} | \mathbf{y}_{1:N}, \theta^{(n)})} d\mathbf{x}_{0:N} \\ &= \int p(\mathbf{x}_{0:N} | \mathbf{y}_{1:N}, \theta^{(n)}) \log p(\mathbf{x}_{0:N}, \mathbf{y}_{1:N} | \theta) d\mathbf{x}_{0:N} \\ & \quad - \int p(\mathbf{x}_{0:N} | \mathbf{y}_{1:N}, \theta^{(n)}) \log p(\mathbf{x}_{0:N} | \mathbf{y}_{1:N}, \theta^{(n)}) d\mathbf{x}_{0:N}. \end{aligned} \quad (99)$$

Note that the latter is independent to θ , it can be omitted [47]. For state estimation, maximizing the loglikelihood of the PDF of observation $\log p(\mathbf{y}_{1:N} | \theta)$, is equivalent to maximize

$$\mathcal{Q}(\theta, \theta^{(n)}) = \mathbb{E} [\log p(\mathbf{x}_{0:N}, \mathbf{y}_{1:N} | \theta) | \mathbf{y}_{1:N}, \theta^{(n)}]. \quad (100)$$

EM algorithm is begin with the initial estimation $\theta^{(0)}$, then iteratively executes E-step and M-step as Algorithm 1.

Algorithm 1 EM algorithm

Require: Initial estimation of parameters $\theta^{(0)}$, error ϵ , maximum iteration number n_m

Ensure: θ^*

1: **repeat**

2: E-step: compute $\mathcal{Q}(\theta, \theta^{(n)})$

3: M-step: $\theta^{(n+1)} \leftarrow \arg \max_{\theta} \mathcal{Q}(\theta, \theta^{(n)})$

4: **until** $|\theta^{(n+1)} - \theta^{(n)}| < \epsilon$, or iteration number is up to n_m

5: **return** $\theta^* \leftarrow \theta^{(n+1)}$

For linear system (1), the probability distribution is

$$p(\mathbf{x}_k | \mathbf{x}_{k-1}) = N(\mathbf{x}_k | A\mathbf{x}_{k-1}, Q), \quad (101a)$$

$$p(\mathbf{y}_k | \mathbf{x}_k) = N(\mathbf{y}_k | C\mathbf{x}_k, R), \quad (101b)$$

$$p(\mathbf{x}_0) = N(m_0, P_0). \quad (101c)$$

With the assumption of Markov property of states, and conditional independence of observations,

$$p(\mathbf{x}_{0:N}, \mathbf{y}_{1:N}) = p(\mathbf{x}_0) \prod_{k=1}^N p(\mathbf{x}_k | \mathbf{x}_{k-1}) \prod_{k=1}^N p(\mathbf{y}_k | \mathbf{x}_k). \quad (102)$$

Hence,

Then, solve equation

$$\frac{\partial \mathcal{Q}(\theta, \theta^{(n)})}{\partial \theta^{(n)}} = 0. \quad (103)$$

For A, C, m_0 , we have,

$$A = \left(\sum_{k=1}^{N-1} \mathbb{E}[\hat{x}_k \hat{x}_{k-1}^T] \right) \left(\sum_{k=1}^{N-1} \mathbb{E}[\hat{x}_{k-1} \hat{x}_{k-1}^T] \right)^{-1}, \quad (104)$$

$$C = \left(\sum_{k=0}^{N-1} y_k \mathbb{E}[\hat{x}_k]^T \right) \left(\sum_{k=0}^{N-1} \mathbb{E}[\hat{x}_k \hat{x}_k^T] \right)^{-1}, \quad (105)$$

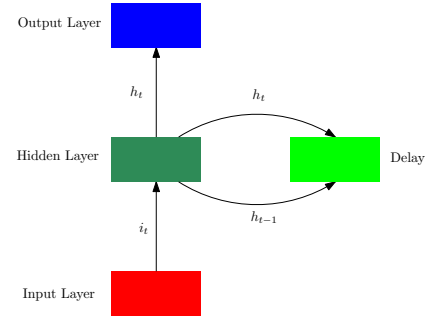


Fig. 3. RNN unit.

$$m_0 = \mathbb{E}[\hat{x}_0]. \quad (106)$$

Then, compute Q, R, P_0 via A, C, m_0 .

$$\begin{aligned} Q &= \frac{1}{N-1} \sum_{k=0}^{N-2} (\mathbb{E}[\hat{x}_{k+1}] - A\mathbb{E}[\hat{x}_k])(\mathbb{E}[\hat{x}_{k+1}] - A\mathbb{E}[\hat{x}_k])^T \\ & \quad + A\text{Var}[\hat{x}_k]A^T + \text{Var}[\hat{x}_{k+1}] \\ & \quad - \text{Cov}(\hat{x}_{k+1}, \hat{x}_k)A^T - A\text{Cov}(\hat{x}_k, \hat{x}_{k+1}), \end{aligned} \quad (107)$$

$$R = \frac{1}{N} \sum_{k=0}^{N-1} [z_k - C\mathbb{E}[\hat{x}_k]][z_k - C\mathbb{E}[\hat{x}_k]]^T + C\text{Var}[\hat{x}_k]C^T, \quad (108)$$

$$P_0 = \mathbb{E}[\hat{x}_0, \hat{x}_0^T] - m_0\mathbb{E}[\hat{x}_0]^T - \mathbb{E}[\hat{x}_0]m_0^T + m_0m_0^T. \quad (109)$$

Here, \hat{x}_k denotes the estimation of Kalman Smoother as Eq. (93).

C. Deep learning for sequential data

In basic feed-forward neural network (FFNN), output of current moment o_t is only determined by input of current moment i_t , which suppress the ability of FFNN to model time-series data. In recurrent neural network (RNN), a delay is used to save the latent state of latest moment h_{t-1} , then, latent state of current moment h_t is determined by both h_{t-1} and i_t . See Fig. 3. [19] suggested that RNN may vanish the gradient as error propagates through time dimension, which leads to long-term dependency problem. Human can selectively remember information. Through gated activation function, LSTM (long short-term memory) model can selectively remember updated information and forget accumulated information.

State estimation can also be seen as estimation on sequences. Recurrent Neural Network (RNN) was adopted for analyzing sequential data, and Long Short-Term Memory (LSTM) [19] model is the most commonly used RNN. Recently, there are many works incorporating LSTM to sequential analysis and state estimation [23], [46]. Subspace learning leads to autoencoder based representation model that incorporating deep learning approaches. Sequence-to-sequence (seq2seq) [49] model adopted autoencoder (i.e. encoder-decoder architecture) for analyzing sequential data.

LSTM introduced gate mechanism in RNN, which can be seen as simulation for human memory, that human can remember useful information and forget useless information.

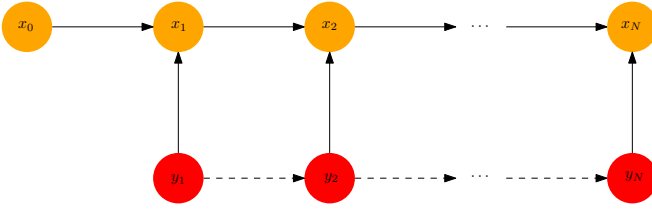
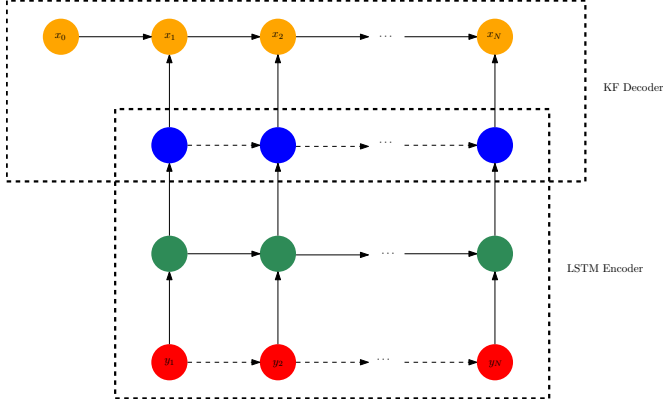
Fig. 4. Basic KF solves x_k via y_k and x_{k-1} .

Fig. 5. LSTM-KF, with LSTM encoder and KF decoder, where dashed lines denote latent connections.

Attention Mechanism [1], [21] can be seen as simulation for human attention, that human can pay attention to useful information and ignore useless information. Transformer [52] is a self-attention based sequence-to-sequence (seq2seq) [49] model to encode and decode sequential data. Bidirectional Encoder Representation Transformer (BERT) with pretraining [13], [22] can perform better than the basic Transformer.

D. Conditional random field based graph neural networks

1) *Conditional random field and state estimation:* [46] suggests that the decoder in seq2seq model can be replaced by Kalman Fiiter. In Fig. 4, Kalman Filter requires input and previous output for current output, which is similar to seq2seq model. Seq2seq suppress the effect of noise through encoder-decoder architecture, which is consistent to the goal of state estimation. Based on deep learning, hidden information of state is depicted more effectively, while the model would not satisfy the assumptions of Markov property of state, along with conditional independence of observation. However, as Fig. 5 shows, Kalman Filter receives the context from LSTM encoder, i.e. observation after LSTM processing. This model is called LSTM-KF.

Based on LSTM-KF, [46] combined LSTM, Transformer and EM-KF, to propose Transformer-KF and Transformer-LSTM-KF (TL-KF). The structures of LSTM-KF, Transformer-KF, and TL-KF, are shown on Fig. 6.

In the proposed TCG-KF model (Transformer-CRF-GNN KF), conditional random field based graph neural networks (CRF-GNN) is proposed to replace vanilla LSTM in TL-KF model, which can fully mine the information of the system. The structure of TCG-KF is shown on Fig. 7.

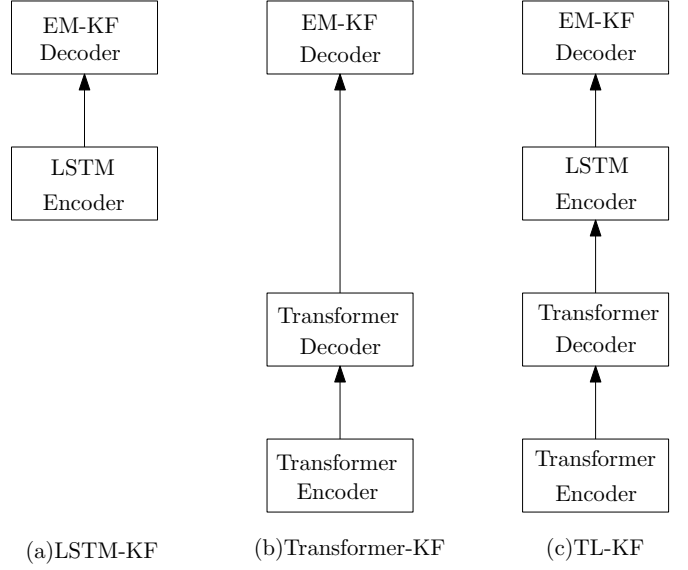


Fig. 6. LSTM-KF, Transformer-KF, and TL-KF for state estimation

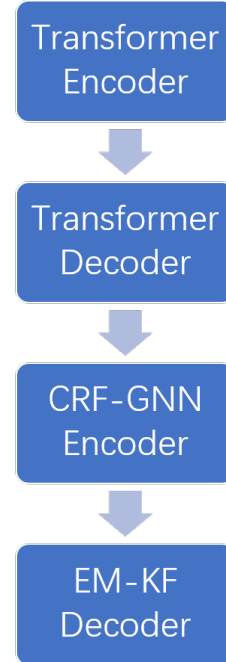


Fig. 7. TCG-KF for state estimation

2) *Conditional random field in machine learning on graph:* In Fig. 5, the factor graph of LSTM Encoder and EM-KF Decoder can be viewed as conditional random field. This can be viewed in the perspective of machine learning on graph.

Consider each node v_i on the graph as a factor x_i in the factor graph, remember $x = (x_1, \dots, x_n)^T$, compatibility function

$$\psi(x) = \exp(-E(x)) \quad (110)$$

Energy function

$$E(x) = \frac{1}{2}(x - \mu)^T Q(x - \mu) \quad (111)$$

Joint probability

$$p(x) = \psi(x)/Z \quad (112)$$

where normalized factor $Z = (2\pi)^{n/2}|Q|^{-1/2}$. Matrix $Q \in \mathbb{R}^{n \times n}$ is precision matrix, i.e. the inverse of covariance matrix. The normalized Laplacian matrix L of a graph can be set as a precision matrix.

[54], [55] solves the weights of edges w_{ij} through quadratic programming problem in local linear embedding (LLE).

$$\begin{aligned} \min_w \varepsilon &= \sum_i \|x_i - \sum_{j: x_j \in N(x_i)} w_{ij} x_j\|^2 \\ \text{s.t.} \quad &\sum_{j: x_j \in N(x_i)} w_{ij} = 1, w_{ij} \geq 0 \end{aligned} \quad (113)$$

In directed graph $w_{ij} \neq w_{ji}$.

$$\begin{aligned} \varepsilon &= \|x_i - \sum_{j: x_j \in N(x_i)} w_{ij} x_j\|^2 \\ &= \left\| \sum_{j: x_j \in N(x_i)} w_{ij} (x_i - x_j) \right\|^2 \\ &= \sum_{j, k: x_j, x_k \in N(x_i)} w_{ij} w_{ik} (x_i - x_j)^T (x_i - x_k) \\ &= \sum_{j, k: x_j, x_k \in N(x_i)} w_{ij} G_{jk}^i w_{ik} \end{aligned} \quad (114)$$

where $G_{jk}^i = (x_i - x_j)^T (x_i - x_k)$ denotes Gram matrix of x_i . When Gram matrix is nearly singular, it can be estimated iteratively.

$$G^{(t+1)} = G^{(t)} + \epsilon \cdot \text{trace}(G) \cdot I, 0 < \epsilon \ll 1 \quad (115)$$

Neighborhood $N(x_i)$ is defined through k-nearest principle. In state estimation or time-series forecasting problem, neighborhood denotes the points in time window, i.e. k-nearest neighborhood when time window width is k.

Theorem 17. *The weights can be solved through*

$$w_{ij} = \frac{\sum_{k \in N(i)} G_{jk}^{-1}}{\sum_{l, s \in N(i)} G_{ls}^{-1}} \quad (116)$$

The analytical solution given above requires the inversion of the Gram matrix, so this calculation method is not robust and requires a large amount of computation. In practical applications, numerical methods are often used to solve quadratic programming problems, such as active set method or interior points method. to solve, or use a solver such as cvxopt. Appendix of proof of Theorem 17 provides a remark w.r.t. an iterative algorithm based on non-negative matrix factorization for solving this quadratic programming problem.

Theorem 18. *For the conditional random field, when the increments are first-order, the energy function is the quadratic form of harmonic operator (normalized Laplacian matrix).*

$$E = \frac{1}{2} x^T L x = \frac{1}{2} \sum_{i,j} w_{ij} (x_i - x_j)^2 \quad (117)$$

Theorem 19. *For the conditional random field, when the increments are second-order, the energy function is the quadratic form of biharmonic operator.*

$$E = \frac{1}{2} x^T L^T L x = -\frac{1}{2} \sum_i \left(\sum_{j \in N_i} (w_{ij} x_j - x_i)^2 \right) \quad (118)$$

Theorem 20. *The expectation for conditional random field to estimate state x from observation y is*

$$\mathbb{E}[x|y] = -Q_{xx}^{-1} Q_{xy} y \quad (119)$$

3) *Proposing GNN in CRF:* For observations y and states of latent variables x in conditional random field (CRF), and according to Markov property in CRF, the state of a node is only related to its neighborhood. Hence, inference and inductive learning procedure on conditional random field as a graph, aggregate messages from neighborhood, which is intrinsically related to graph neural networks.

Currently, there has been a series of works combining variational inference with machine learning on graphs [40], [55]. Because variational inference needs to be modeled by conditional random fields (CRFs), it is natural to treat CRFs as graphs.

Consider the process of sampling $q(z)$ from $p(z, x)$. Assuming that the hidden variable on the node k on the graph is z_k , by the mean field theory

$$q(z) = \prod_k q(z_k) \quad (120)$$

by the chain rule of conditional probability

$$p(z, x) = p(x) \prod_k p(z_k | z_{n \setminus k}, x) \quad (121)$$

Where $n \setminus k$ represents the set of all nodes on the graph except node k , so optimizing ELBO is equivalent to optimizing

$$\begin{aligned} L &= \log p(x) + \sum_k q(z_k) \mathbb{E}_{q(z_{n \setminus k})} [\log p(z_k | z_{n \setminus k}, x)] \\ &\quad - \sum_k \mathbb{E}_{q(z_k)} [\log q(z_k)] \end{aligned} \quad (122)$$

Derivation of the functional L using the variational method

$$\frac{\partial L}{\partial q(z_k)} = \mathbb{E}_{q(z_{n \setminus k})} [\log p(z_k | z_{n \setminus k}, x)] - \log q(z_k) - 1 = 0 \quad (123)$$

have to

$$\log q(z_k) = \mathbb{E}_{q(z_{n \setminus k})} [\log p(z_k | z_{n \setminus k}, x)] + \text{const} \quad (124)$$

This means that

$$q(z_k) \propto \exp \left(\mathbb{E}_{q(z_{n \setminus k})} [\log p(z_k | z_{n \setminus k}, x)] \right) \quad (125)$$

This means that we need to sample from all nodes in the graph except node k to find $q(z_k)$. This will be very troublesome when the number of nodes in the whole graph is large.

Theorem 21. *The process of obtaining $q(z_k)$ by sampling from all nodes on the graph except node k , you can obtain $q(z_k)$ by sampling from the neighborhood $N(k)$ of node k to replace [40], [55], that is*

$$q(z_k) \propto \exp \left(\mathbb{E}_{q(z_{N(k)})} [\log p(z_k | z_{N(k)}, x)] \right) \quad (126)$$

According to the mean field assumption, that is, the hidden variables are independent of each other, and there are

$$q(z_k) \propto \exp \left(\mathbb{E}_{q(z_{N(k)})} [\log p(z_k, z_{N(k)}, x)] \right) \quad (127)$$

In other words, it is also possible to sample from the joint distribution of node k and its neighbors $N(k)$.

The formula of the l -th ($l > 0$) graph convolutional layer is

$$H^{(l)} = \rho(\tilde{D}^{-1/2} \tilde{A} \tilde{D}^{-1/2} H^{(l-1)} \Theta^{(l)}), \quad (128)$$

where \tilde{A} is adjacency matrix with self-loop, i.e. $\tilde{A} = A + I$. \tilde{D} is a diagonal matrix called degree matrix, $\tilde{D}_{ii} = \sum_j \tilde{A}_{ij}$, $\rho(\cdot)$ denotes nonlinear activation function, $\Theta^{(l)}$ denotes weight of the l -th layer of network, and $H^{(0)}$ is the initial input feature matrix. Let $\hat{A} = \tilde{D}^{-1/2} \tilde{A} \tilde{D}^{-1/2}$, then

$$H^{(l)} = \rho(\hat{A} H^{(l-1)} \Theta^{(l)}) \quad (129)$$

denotes first-order aggregation, while

$$H^{(l)} = \rho(\hat{A}^2 H^{(l-1)} \Theta^{(l)}) \quad (130)$$

denotes second-order aggregation. For CRF-GNN, the message passing procedure of GNN is illustrated as the following formula:

$$\bar{\mathbf{h}}_i^{(k)} \leftarrow \frac{1}{d_i + 1} \mathbf{h}_i^{(k-1)} + \sum_{j=1}^n \frac{1}{\sqrt{(d_i + 1)(d_j + 1)}} \mathbf{h}_j^{(k-1)} \quad (131)$$

4) *Inductive learning*: The CRF algorithm on graph is easy to implement inductive learning. For a new point x_o

$$\mathbb{E}[x_o|x] = -q_o^{-1} q_{on} y \quad (132)$$

where $q_{on} = (q_{o1}, q_{o2}, \dots)$.

If states are biased,

$$x - b_x \sim N(0, 1/\lambda) \quad (133)$$

where $0 < \lambda < 1$, then suppose

$$\ddot{x}_i \sim N(0, 1/(1 - \lambda)) \quad (134)$$

For joint distribution $p(y, x, b_x)$

$$Q = (1 - \lambda) \begin{pmatrix} Q_{yy} & Q_{yx} & 0 \\ Q_{xy} & Q_{xx} & 0 \\ 0 & 0 & 0 \end{pmatrix} + \lambda \begin{pmatrix} 0 & 0 & 0 \\ 0 & I & -I \\ 0 & -I & I \end{pmatrix} \quad (135)$$

i.e.

$$Q = \begin{pmatrix} (1 - \lambda)Q_{yy} & (1 - \lambda)Q_{yx} & 0 \\ (1 - \lambda)Q_{xy} & (1 - \lambda)Q_{xx} + \lambda I & -\lambda I \\ 0 & -\lambda I & \lambda I \end{pmatrix} \quad (136)$$

Then, calculate $\mathbb{E}(x|y, b_x)$ is equivalent to solve linear equation

$$\begin{pmatrix} (1 - \lambda)Q_{yy} & (1 - \lambda)Q_{yx} & 0 \\ (1 - \lambda)Q_{xy} & (1 - \lambda)Q_{xx} + \lambda I & -\lambda I \\ 0 & -\lambda I & \lambda I \end{pmatrix} \begin{pmatrix} y \\ x \\ b_x \end{pmatrix} = 0 \quad (137)$$

This problem can be relaxed into linear least square problem.

If observations are biased,

$$y - b_y \sim N(0, \lambda) \quad (138)$$

By $\ddot{x}_i \sim N(0, 1/(1 - \lambda))$, for $p(y, x, b_y)$

$$Q = (1 - \lambda) \begin{pmatrix} Q_{yy} & Q_{yx} & 0 \\ Q_{xy} & Q_{xx} & 0 \\ 0 & 0 & 0 \end{pmatrix} + \lambda \begin{pmatrix} I & 0 & I \\ 0 & 0 & 0 \\ -I & 0 & I \end{pmatrix} \quad (139)$$

i.e.

$$Q = \begin{pmatrix} (1 - \lambda)Q_{yy} + \lambda I & (1 - \lambda)Q_{yx} & -\lambda I \\ (1 - \lambda)Q_{xy} & (1 - \lambda)Q_{xx} & 0 \\ -\lambda I & 0 & \lambda I \end{pmatrix} \quad (140)$$

Then calculate $\mathbb{E}(x, y|b_y)$ is equivalent to

$$\begin{pmatrix} (1 - \lambda)Q_{yy} + \lambda I & (1 - \lambda)Q_{yx} & -\lambda I \\ (1 - \lambda)Q_{xy} & (1 - \lambda)Q_{xx} & 0 \\ -\lambda I & 0 & \lambda I \end{pmatrix} \begin{pmatrix} y \\ x \\ b_y \end{pmatrix} = 0 \quad (141)$$

5) *Modification of models for state estimation*: The input of the Transformer is a two-dimensional matrix of data at intervals of a period of time, with a size of TimeWindow \times Features. In numerical simulation on mobile robot model, the feature dimension is 3, including the values of displacement, velocity and acceleration. In Empirical studies on stock prediction, features include the basic stock market data (opening price, closing price, highest price, lowest price, trading volume), as well as the ten technical indicators introduced in Appendix (DIF, DEM, MACD Histogram, RSI, K, D, J, ROC, ATR, OBV). The feature dimension is 15.

In LSTM, we adopted look back trick for time-series forecasting, and the look back number is 5, i.e. o_t can be obtained through o_{t-1}, \dots, o_{t-5} . This means that the TimeWindow width is 5. The layer number of LSTM is 3, and the size is 10. The train set and test set was divided at 9:1. The epoch number is 100.

Basic Transformer is designed for natural language processing. To adopt Transformer for processing time-series data directly, there are some settings that need to be operated. The hidden dimension of self-attention layer is the length of sequence N . The hidden dimension of FFNN layer is $4N$. The dimension of input λ is the dimension of observation. The dimension of model $d = 512$. Transformer is trained by introducing dropout [48], and the dropout rate is 0.1. The head number is 4, and the epoch number is 500.

The experiments are implemented on Python 3.7.1, with Anaconda 5.3.1 and Pytorch 1.0. The codes are run on an NVIDIA GTX2070 GPU with 8GB memory. The model is trained through Adam optimizer [27], and learning rate is 0.1.

V. EXPERIMENTS

A. Node classification for text classification

Cora dataset [43] has a total of 2708 sample points, each sample point is a paper, and all sample points are divided into 7 categories. Each paper is represented by a 1433-dimensional word vector to represent its feature vector. Each element of the word vector corresponds to a word, and the element has only two values of 0 or 1. Take 0 to indicate that the word corresponding to this element is not in the paper, and take 1 to indicate that it is in the paper. The citation relationship of the paper is the edge of the graph, and there

TABLE I
COMPARISON ON TEXT CLASSIFICATION

Method	Cora	MR
GCN	0.8150	0.7552
MPNN	0.8040	0.7436
GraphSAGE	0.8220	0.7642
GAT	0.8300	0.7665
AGNN	0.8280	0.7633
POGNN	0.8350	0.7692

are no isolated points on the graph. Only a small number of sample points (140 points) in the dataset are labeled with class labels, so the classification problem belongs to semi-supervised classification.

MR (Sentiment polarity dataset from Movie Review) dataset [61] is a sentiment dataset based on movie reviews. Each sample point can be a movie review, or a sentence or a segment. Each sample is labeled as positive sentiment or negative sentiment, so the classification problem is a binary classification problem. We form a graph of 29,426 nodes from 10,662 articles and 18,764 keywords. The initial features of nodes are one-hot features, which are mapped to a 300-dimensional vector by Word2Vec.

The proposed POGNN is compared with graph convolutional networks (GCN) [28], GraphSAGE [20], MPNN (message passing network) [18], graph attention networks (GAT) [53], and attention-based graph neural networks (AGNN) [50]. Table I shows that the proposed POGNN outperforms all compared methods.

B. Graph classification for protein classification

Definition 8 (Designing protein graph through secondary structure elements). *Borgwardt et al. [6] designed protein graph models to contain information about structure, sequence and chemical properties of a protein. For this purpose, each graph represents exactly one protein. Nodes in graph represent secondary structure elements (SSEs) within the protein structure, i.e. helices, sheets and turns. 85% of secondary structure elements are in these three categories: α -helix, β -sheet and β -turn. In addition to the above regular conformations, some irregular conformations of the peptide plane in the polypeptide chain are called random coil. Node feature vector is the one-hot encoding of these three categories SSEs: α -helix, β -sheet and β -turn. Edges connect nodes if those are neighbors along the AA sequence or if they are neighbors in space within the protein structure. When two nodes are less than a threshold measured by angstroms apart, connect them with an edge. Borgwardt et al. [6] proposed ENZYMES dataset and PROTEINS dataset for protein classification.*

Definition 9 (Designing protein graph through amino acid embedding). *D&D dataset [14] is a dataset containing 1178 proteins. To designed protein graph models to contain information about structure, sequence and chemical properties of a protein, each graph represents exactly one protein. Nodes in graph represent amino acids. Node embedding contains information about residue, sequence and chemical properties*

of an amino acid, and the dimension is 89. When two nodes are less than a threshold measured by angstroms apart 6 angstroms apart (i.e. 6×10^{-10} meters), connect them with an edge.

Table II lists the situation on protein classification datasets [6], where AvgNodes & AvgEdges denote the average NodeNumber and EdgeNumber of graphs in the datasets. ENZYMES is a 6-class classification dataset with 600 graphs, each class contains 100 graphs. The protein classification datasets, as well as other graph classification datasets towards compounds etc., can be downloaded from (<https://ls11-www.cs.tu-dortmund.de/people/morris/graphkerneldatasets/>) or (<https://chrsmrrs.github.io/datasets/docs/datasets/>).

Predicting whether these proteins are enzymes in D&D dataset [14] is a binary classification problem. VSPool is compared with GCN [28] with mean pooling, GIN [59] with mean pooling, Diffpool [62], EigenPool [36], graph u-net [16], and SAGPool [30]. Table III shows that the proposed VSPool outperforms all compared methods.

C. State estimation for robotics

Consider a linear mobile robot model on one DOF, with displacement, velocity and acceleration as state variables. In actual nonlinear robot systems, dynamic equations can usually be linearized through second-order derivative of displacement. So a linear mobile robot model on one DOF, with displacement, velocity and acceleration, is essential as the beginning of studying the complicated nonlinear robot systems. Based on classical computer vision theory, displacement is observed by Efficient Perspective-n-Points (EPnP) algorithm. [2], [31]

$$\begin{cases} x_k = x_{k-1} + v_{k-1}T + \frac{1}{2}a_{k-1}T^2 \\ v_k = v_{k-1} + a_{k-1}T \end{cases}, k = 1, 2, \dots, N. \quad (142)$$

Here, T denotes a sample term following Shannon's sampling theorem. Suppose only displacement can be observed, thus,

$$\begin{pmatrix} x_k \\ v_k \\ a_k \end{pmatrix} = \begin{pmatrix} 1 & T & 0.5T^2 \\ 0 & 1 & T \\ 0 & 0 & 1 \end{pmatrix} \begin{pmatrix} x_{k-1} \\ v_{k-1} \\ a_{k-1} \end{pmatrix} + w_k, \\ y_k = \begin{pmatrix} 1 & 0 & 0 \end{pmatrix} x_k + v_k, \\ w_k \sim N(0, Q), v_k \sim N(0, R), x_0 \sim N(m_0, P_0). \quad (143)$$

As Q, R, m_0, P_0 were unknown, we first adopted EM algorithm for estimating R , then new series for estimating Q, m_0, P_0 were generated, to compare EM-KF, LSTM-KF, Transformer-KF and TL-KF. Suppose Q, R, P_0 are as form $\sigma^2 I$, and m_0 is as form $(0, 0, m_a)^T$. The σ^2 estimation is the quotient of the trace of covariance matrix and order of matrix, and m_{03} is the estimation of m_a .

The iteration number of EM algorithm is 10. The de facto values $Q = 1 \times 10^{-2} I_3, R = 5 \times 10^{-3} I_1, m_0 = (0, 0, 0.1)^T, P_0 = 0.1 I_3$, sampling term $T = 0.01$ second, sequence length $N = 200$. At the beginning, we set $Q = 2 \times 10^{-2} I_3, R = I_1, m_0 = (0, 0, 1)^T, P_0 = 5 I_3$.

TABLE II
SITUATION ON PROTEIN CLASSIFICATION DATASETS

Name	GraphNum	ClassNum	PosNum	NegNum	NodeFeatDim	AvgNodes	AvgEdges
D&D	1178	2	691	487	89	284.32	715.66
PROTEINS	1113	2	663	450	3	39.06	72.82
ENZYMES	600	6	-	-	3	32.63	62.14

TABLE III
COMPARISON ON PROTEIN CLASSIFICATION OF D&D DATASET

Method	Acc
WL Graph Kernel	0.7834
GCN	0.7590
GIN	0.7530
DiffPool	0.8064
EigenPool	0.7860
Graph U-Nets	0.8243
SAGPool	0.7707
VSPool	0.8275

TABLE IV
COMPARISON ON PARAMETERS ESTIMATION.

	σ_q^2	σ_r^2	m_a	σ_p^2
actual values	1.0×10^{-2}	5.0×10^{-3}	0.1	0.1
EM-KF	2.04×10^{-2}	4.23×10^{-3}	0.879	0.417
LSTM-KF	0.14×10^{-2}	34.3×10^{-3}	0.109	0.116
Transformer-KF	1.18×10^{-2}	98.4×10^{-3}	0.768	0.359
TL-KF	1.27×10^{-2}	44.8×10^{-3}	0.121	0.118
TCG-KF	1.07×10^{-2}	4.84×10^{-3}	0.096	0.115

Table IV gives the results of parameter estimation using these methods. TCG-KF gives more accurate estimates of parameters.

Table V gives a comparison of the accuracy between the above methods and the basic Kalman Filter (that is, filtering directly with the initial guess of the parameter values). It can be seen that for the system shown in (143) and the initial values of system parameter iteration given in this paper, the accuracy of using EM-KF algorithm is not significantly different from that of using Kalman Filter directly. After using LSTM or Transformer to process the observation sequence, the errors can be significantly reduced. And TCG-KF is superior to current methods.

D. State estimation for stock prediction

Classical stock prediction methods are based on ARMA (Auto Regressive Moving Average) model and ARIMA

TABLE V
COMPARISON ON STATE ESTIMATION, WHERE MSE DENOTES MEAN SQUARE ERROR.

	Filter MSE(m^2)	Smoother MSE(m^2)
KF	26.83×10^{-3}	16.95×10^{-3}
EM-KF	26.32×10^{-3}	15.19×10^{-3}
LSTM-KF	17.51×10^{-3}	11.52×10^{-3}
Transformer-KF	9.05×10^{-3}	6.55×10^{-3}
TL-KF	5.07×10^{-3}	4.89×10^{-3}
TCG-KF	3.37×10^{-3}	2.85×10^{-3}

(Auto Regressive Integrated Moving Average) model. An ARMA(p,q) model

$$s_t = a_0 + \sum_{i=1}^p a_i s_{t-i} + w_t + \sum_{i=1}^q b_i w_{t-i}, \quad (144)$$

where a,b are parameters, w is noise. ARMA model can be used when sequence $s_{1:N}$ is stationary, which means

$$\mathbb{E}[s_t] = \text{Constant}. \quad (145)$$

$$\text{Cov}(s_t, s_{t-k}) = \text{Constant}. \quad (146)$$

where $t = 1, 2, \dots, N$ and $k = 1, 2, \dots, t$.

When sequence is non-stationary, ARIMA(p,q,d) adopts d -order difference to the sequence. In stock prediction, the first-order difference $x_{1:N} = \hat{s}_{1:N}$ (i.e. $x_k = s_k - s_{k-1}$) is usually considered as stationary sequence.

After applying long short-term memory to our predicting model, the linear system can be simply defined as:

$$\begin{cases} x_k = x_{k-1} + N(0, 1) \\ y_k = x_k + N(0, 1) \end{cases}, k = 1, 2, \dots, N. \quad (147)$$

The evaluation metrics are mean absolute error (MAE), root of mean square error (RMSE) and mean absolute percentage error (MAPE).

$$MAE = \frac{1}{n} \sum_{t=1}^n |\hat{X}_t - X_t| \quad (148)$$

$$RMSE = \sqrt{\frac{1}{n} \sum_{t=1}^n (\hat{X}_t - X_t)^2} \quad (149)$$

$$MAPE = \frac{1}{n} \sum_{t=1}^n \left| \frac{\hat{X}_t - X_t}{X_t} \right| \quad (150)$$

The data used in this article comes from the open and free public dataset in Tushare (<https://www.tushare.pro/>) for the research of stock market in China, which has the characteristics of rich data, simple use, and convenient implementation. It is very convenient to obtain the basic market data of stocks by calling the API.

In order to test the predictive ability of the model, this paper selects three representative stocks in the market for empirical analysis. See Table VI. The data is selected from the data from January 1, 2004 to October 1, 2019, the data in one day denotes a point of the sequence.

The compared methods include:

- ARIMA
- ARIMA-NN: Zhang [63] improved time-series forecast-
ing using a hybrid ARIMA and neural network model.

TABLE VI
BASIC SITUATION OF STOCK DATASETS, WHERE (P,Q,D) DENOTES THE
BASIC ARIMA PARAMETERS USED FOR COMPARISON

	Stock code in China stock market	Sequence length	(p,q,d)
Stock 1	000001	3678	(4,1,2)
Stock 2	600030	3740	(2,1,3)
Stock 3	600036	3757	(1,1,1)

TABLE VII
RESULTS ON STOCK 1

	MAE	RMSE	MAPE
ARIMA	0.2956	0.3693	0.0177
ARIMA-NN	0.4269	0.4768	0.0255
LSTM-KF	0.2574	0.3211	0.0162
Transformer-KF	0.1978	0.2677	0.0145
TL-KF	0.1889	0.2546	0.0132
TCG-KF	0.1627	0.2118	0.0102

- LSTM-KF, Transformer-KF, TL-KF and TCG-KF is proposed by our work.

Table VII, VIII, IX demonstrate that the proposed the conditional random field and Transformer-based graph neural networks for Kalman filter in state estimation, outperforms current methods.

VI. CONCLUSIONS

Probabilistic theory and differential equation are powerful tools for the interpretability and guidance of the design of deep learning models on graphs of learning latent variables from observations. This paper concentrates on state estimation and subspace learning in latent variable learning. State estimation solves optimal value for latent variable from noised observation. Subspace learning maps high-dimensional features on low-dimensional subspace to capture efficient representation. Inspired by probabilistic theory and differential equations, this paper proposes graph neural networks to solve state estimation

TABLE VIII
RESULTS ON STOCK 2

	MAE	RMSE	MAPE
ARIMA	0.2396	0.2685	0.0105
ARIMA-NN	0.2748	0.2953	0.0121
LSTM-KF	0.1662	0.2033	0.0078
Transformer-KF	0.1670	0.1923	0.0075
TL-KF	0.1421	0.1884	0.0070
TCG-KF	0.1226	0.1707	0.0063

TABLE IX
RESULTS ON STOCK 3

	MAE	RMSE	MAPE
ARIMA	0.3592	0.5080	0.0091
ARIMA-NN	0.4201	0.5567	0.0116
LSTM-KF	0.3213	0.3719	0.0091
Transformer-KF	0.3137	0.3442	0.0081
TL-KF	0.3021	0.3314	0.0079
TCG-KF	0.2774	0.3208	0.0070

and subspace learning problems. This paper conducts theoretical studies, and adopts empirical studies on several tasks, including text classification, protein classification, stock prediction and state estimation for robotics. Experiments demonstrate that the proposed graph neural networks are superior to the current methods.

APPENDIX A

SUMMARY OF SUBSPACE LEARNING ALGORITHMS

1) Low Rank Representation

- **Measurement** $\min_Z \text{rank}(Z)$ s.t. $X = XZ$
- **Convex Surrogate** $\min_{Z,E} \|Z\|_* + \lambda \|E\|_{2,1}$ s.t. $X = XZ + E$
- **Methods** ALM, APG, ADMM, LADMAP

2) Matrix Completion

- **Measurement** $\min_M \text{rank}(M)$ s.t. $P_\Omega(M) = P_\Omega(A)$
- **Convex Surrogate** $\min_M \|M\|_*$ s.t. $P_\Omega(M) = P_\Omega(A)$
- **Methods** APG

3) Principal Component Analysis (PCA)

- **Measurement** $\max_W \text{trace}(W^T X X^T W)$ s.t. $W^T W = I$
 - i.e. $\min_{W,H} \|X - WH\|_F^2$ s.t. $W^T W = I$
 - Minimum projection distance of the samples
 - Maximum projection variance of the samples
 - PCA is a low rank model $\min_{L: \text{rank}(L) \leq k} \|X - L\|_F^2$, thus it equals singular value thresholding in its result.
- **Methods** Eigenvalue Decomposition

4) Linear Discriminant Analysis (LDA)

- **Measurement** $\max_W \text{trace}(W^T S_b W) / \text{trace}(W^T S_w W)$
- **Methods** Generalized Eigenvalue Decomposition

5) Robust PCA

- **Measurement** $\min_{L,S} \|L\|_* + \rho \|S\|_1$ s.t. $M = L + S$
- **Methods** ADMM, here it calls robust principal component pursuit (RPCP)

6) Sparse Subspace Clustering

- **Measurement** $\min_Z \|Z\|_0$ s.t. $X = XZ$
- **Convex Surrogate** $\min_Z \|Z\|_1$ s.t. $X = XZ$
- **Methods** ALM, APG

7) Sparse Coding

- **Measurement** $\min_{D,X} \|Y - DX\|_F^2 + \lambda \|X\|_1$, usually calls LASSO (Least Absolute Shrinkage and Selection Operator).
- **Methods** ADMM
 - Update X , called sparse coding, and methods include match pursuit (a kind of greedy algorithm), ISTA, FISTA etc.
 - Update D , called dictionary learning, usually use Method of Optimal Directions (MOD) or K-SVD

8) Normalized Cuts / Laplacian Eigenmaps / Spectral Clustering

- **Measurement** $\min_y y^T L y$, where L denotes normalized Laplacian Matrix.
- **Methods** Eigenvalue Decomposition, the second smallest eigenvector of L is the real valued solution, since the smallest eigenvalue of L is 0 with an all-one eigenvector.

9) Non-negative matrix factorization (NMF)

- **Measurement** $\min_{W \geq 0, H \geq 0} D[X||WH]$, where $D[A||B]$ denotes the divergence between A and B
 - Frobenius divergence, $D[X||WH] = \|X - WH\|_F^2$, is a maximum likelihood estimator due to the additive Gaussian noise, usually used.
 - KL divergence, $D[X||WH] = \sum_{i,j} X_{ij} \ln X_{ij}/(WH)_{ij} - X_{ij} + (WH)_{ij}$, is maximum likelihood for the Poisson process.
 - Graph NMF, $\min_{U \geq 0, V \geq 0} \|X - UV^T\|_F^2 + \text{trace}(VLV^T)$
- **Methods** Multiply Iteration

10) Local Linear Embedding (LLE)

- **Measurement** $\min \text{trace}(ZQZ^T)$ s.t. $ZZ^T = I$, where $Q = (I - W)^T(I - W)$, and here the normalized Laplacian is $L = I - W$.
- **Methods** Eigenvalue Decomposition

11) Support Vector Machine (SVM)

- **Measurement** Maximize the margin
 - Kernel SVM, the primal problem is $\min_{w,b} \frac{1}{2} \|w\|^2$ s.t. $y_i(w^T f(x_i) + b) \geq 1$. The dual problem is $\max_{\alpha} \sum_i \alpha_i - \frac{1}{2} \sum_{i,j} \alpha_i \alpha_j y_i y_j \kappa(x_i, x_j)$ s.t. $\sum_i \alpha_i y_i = 0, \alpha_i \geq 0$, where kernel function $\kappa(x_i, x_j) = f^T(x_i) f(x_j)$.
 - Soft margin SVM, $\max_{\alpha} \sum_i \alpha_i - \frac{1}{2} \sum_{i,j} \alpha_i \alpha_j y_i y_j \kappa(x_i, x_j)$ s.t. $\sum_i \alpha_i y_i = 0, C \geq \alpha_i \geq 0$, equivalent to $\min_{\alpha, \xi} C \sum_i \xi_i + \gamma \alpha^T K \alpha$ s.t. $y_i(\sum_j \alpha_j \kappa(x_i, x_j) + b) \geq 1 - \xi_i, \xi_i \geq 0$
 - Transductive SVM is applied to solve semi-supervised learning problem. The key idea is to assign a pseudo-label to each unlabeled data first, then iteratively correct the labels.
 - Laplacian SVM, suppose u and l denote number of unlabeled and labeled data, optimize $\min_{\alpha, \xi} \frac{1}{l} \sum_i^l \xi_i + \gamma \alpha^T K \alpha + \frac{\lambda}{(u+l)^2} \alpha^T K L K \alpha$ s.t. $y_i(\sum_j^{l+u} \alpha_j \kappa(x_i, x_j) + b) \geq 1 - \xi_i, \xi_i \geq 0$
- **Methods** Sequential Minimum Optimization (SMO)

12) Multiple Dimensional Scaling (MDS) / IsoMAP (Isometric Feature Mapping)

- **Measurement** $\min_Y \|G - Y^T Y\|_F^2$, where $G_{ij} = \langle x_i, x_j \rangle$ is the Gram matrix, that can be computed from pairwise distances.
- PCA and MDS are in some sense dual to each other. Suppose $X \in \mathbb{R}^{D \times N}$, in PCA, we compute the $D \times D$ covariance matrix XX^T , In MDS, we compute the $N \times N$ Gram matrix. For Euclidean

distances, the two methods yield the same embedding results (up to an arbitrary rotation).

- In IsoMAP we use geodesic distances rather than Euclidean distances in MDS. After constructing a graph, we apply Dijkstra all-pairs shortest-paths algorithm to compute the distances.

- **Methods** Eigenvalue Decomposition of Gram matrix, $G = V \Lambda V^T$, then $Y^* = \Lambda^{1/2} V^T$.

13) Label Propagation (LP)

- **Measurement** $\min_F F^T L F + \gamma \|F - Y\|_F^2$, considering normalized Laplacian is $L = I - W$, the optimal solution is $F^* = (1 - \alpha)(I - \alpha W)^{-1} Y$, where $\alpha = 1/(1 + \gamma)$.
- **Methods** Iteration $F^{(k)} = \alpha W F^{(k-1)} + (1 - \alpha) Y, 0 < (1 - \alpha) \ll 1$.

14) Regularized Least Square (RLS)

- **Measurement** Minimize Mean Square Errors
 - Tikhonov Regularization, $\min_x \|Ax - b\|_2^2 + \lambda \|x\|_2^2 \Rightarrow x^* = (A^T A + L^T L)^{-1} A^T b$, also calls ridge regression.
 - Laplacian RLS, $\min_F F^T L F + \gamma \|F - Y\|_F^2 + \lambda \|F\|_F^2$, the optimal solution is $F^* = (1 - \alpha)(I - \alpha W)^{-1} Y$, where $\alpha = 1/(1 + \gamma + \lambda)$.

15) Probabilistic Matrix Factorization (PMF)

- **Measurement** $\min_{U,V} \|R - U^T V\|_F^2$ s.t. $P_{\Omega}(R) = P_{\Omega}(U^T V)$, where $R \sim N(U^T V, \sigma^2 I), U \sim N(0, \sigma_U^2 I), V \sim N(0, \sigma_V^2 I)$, $\max_{U,V} \ln p(U, V|R)$ equals to $\min_{U,V} \frac{1}{2} P_{\Omega}(\|R - U^T V\|_F^2) + \frac{\lambda_U}{2} \|U\|_F^2 + \frac{\lambda_V}{2} \|V\|_F^2$, it is regularized SVD where $\lambda_U = \sigma^2/\sigma_U^2, \lambda_V = \sigma^2/\sigma_V^2$.

APPENDIX B PROOF OF THEOREMS

Proof of Theorem 1

Proof.

$$\Delta(y) = \nabla \cdot \nabla y = \text{div} \nabla y, \quad \int_M \langle X, \nabla y \rangle = \int_M \text{div}(X) y \quad (151)$$

So

$$\int_M \|\nabla y\|^2 = \int_M \Delta(y) y \quad (152)$$

So

$$\min y^T \Delta y \Leftrightarrow \min \|\nabla y\|^2 \quad (153)$$

□

Proof of Theorem 2

Proof. We regard the label information as the temperature on the graph. When the "thermal equilibrium" is reached, that is, when the label propagation converges, there will be $\Delta u = 0$. Let $u(x, 0) = f(x)$ be the initial heat distribution, and solve the problem of partial differential equation (11) according to this initial condition, which is called the Cauchy problem of

heat conduction equation. The special solution of (11) when $f(x) = \delta(x)$ is

$$\Phi_t(x) = \frac{1}{(4\pi t)^{n/2}} \exp\left(-\frac{\|x\|^2}{4t}\right), t > 0 \quad (154)$$

This is also known as the fundamental solution of the heat conduction equation, and

$$\int_{\mathbb{R}^n} \Phi_t(x) dx = 1 \quad (155)$$

Let $H_t(x, y) = \Phi_t(x - y)$, the solution of (11) is

$$u(x, t) = \int_M H_t(x, y) f(y) dy \quad (156)$$

That is, the convolution of the kernel H_t and the initial condition $f(x)$. so

$$\begin{aligned} \Delta f(x) &= \frac{\partial}{\partial t} \left(\int_M H_t(x, y) f(y) dy \right) \Big|_{t \rightarrow 0} \\ &= -\frac{1}{t} (f(x) - g(x, y)) \end{aligned} \quad (157)$$

$$g(x, y) = (4\pi t)^{-n/2} \int_M \exp\left(-\frac{\|x - y\|^2}{4t}\right) f(y) dy \quad (158)$$

For a point x_i , assuming that there are k points in its neighborhood, then

$$\Delta f(x_i) = -\frac{1}{t} (f(x_i) - g(x_i, x_j)) \quad (159)$$

$$g(x_i, x_j) = \frac{1}{k} (4\pi t)^{-n/2} \sum_{j \in N(i)} \exp\left(-\frac{\|x_i - x_j\|^2}{4t}\right) f(x_j) \quad (160)$$

where $N(i) = \{x_j | 0 < \|x_i - x_j\| < \varepsilon\}$, when $\Delta f(x_i) \approx 0$

$$\frac{1}{k} (4\pi t)^{-n/2} \sum_{j \in N(i)} \exp\left(-\frac{\|x_i - x_j\|^2}{4t}\right) = 1 \quad (161)$$

so

$$w_{ij} = \exp\left(-\frac{\|x_i - x_j\|^2}{4t}\right) \quad (162)$$

□

Proof of Theorem 3

Proof. Consider the iterative process of label propagation $y^{(t)} = \alpha W y^{(t-1)} + (1 - \alpha) y^{(0)}$, $\alpha \approx 1$, then

$$\begin{pmatrix} y_u^{(t)} \\ y_l^{(t)} \end{pmatrix} \approx \begin{pmatrix} W_{uu} & W_{ul} \\ W_{lu} & W_{ll} \end{pmatrix} \begin{pmatrix} y_u^{(t-1)} \\ y_l^{(t-1)} \end{pmatrix} \quad (163)$$

$$y_u^{(t)} \approx W_{uu} y_u^{(t-1)} + W_{ul} \bar{y}_l \quad (164)$$

The general solution to this difference equation is

$$y_u^{(t)} = W_{uu}^t y_u^{(0)} + \left(\sum_{i=1}^t W_{uu}^{i-1} \right) W_{ul} \bar{y}_l \quad (165)$$

Because the spectral radius $\rho(W_{uu}) < 1$, so $\lim_{t \rightarrow +\infty} W_{uu}^t = 0$ (this shows that the final estimation result of y_u^0 has little effect, usually set $y_u^0 = 0$), and because $\lim_{t \rightarrow +\infty} \sum_{i=1}^t W_{uu}^{i-1} = (I - W_{uu})^{-1}$, so

$$y_u^* = (I - W_{uu})^{-1} W_{ul} \bar{y}_l. \quad (166)$$

And because $Q = I - W$, so $Q_{uu} = I - W_{uu}$, $Q_{ul} = -W_{ul}$, namely $y_u^* = -Q_{uu}^{-1} Q_{ul} \bar{y}_l$. □

Proof of Theorem 6

Proof. $\rho(D^{-1}A) = 1$, so the eigenvalue of $D^{-1}A$ is located in the $[-1, 1]$ interval, obviously, for (the number of nodes For any graph not less than 2), $D^{-1}A$ has an eigenvalue of 1, and the corresponding eigenvector is

$$(1, 1, \dots, 1)^T$$

Only for the bipartite graph, $D^{-1}A$ has the eigenvalue -1 , assuming that the two parts of the bipartite graph have a, b nodes respectively, then the eigenvalue -1 corresponds to The eigenvector is

$$\underbrace{(1, 1, \dots, 1)}_a, \underbrace{(-1, -1, \dots, -1)}_b^T$$

And because

$$\frac{x^T L_{rw} x}{x^T x} = 1 - \frac{x^T D^{-1} A x}{x^T x} \quad (167)$$

So we can get Theorem. □

Proof of Theorem 7

Proof. Notice that

$$\rho(\tilde{D}^{-1/2} A \tilde{D}^{-1/2}) = \frac{d_m}{d_m + 1}$$

so

$$\min_{\|x\|=1} x^T \tilde{D}^{-1/2} A \tilde{D}^{-1/2} x \geq -\frac{d_m}{d_m + 1}$$

From this, we can directly get

$$\tilde{\lambda}_n \leq 1 - \frac{1}{d_m + 1} - \left(-\frac{d_m}{d_m + 1} \right) = \frac{2d_m}{d_m + 1}$$

This approximation can significantly reduce the amount of computation for $\tilde{\lambda}_n$, in fact, \tilde{d} is the quotient of the total number of edges divided by the total number of nodes, in other words, the sum of adjacency matrix elements divided by the matrix order 's business.

For undirected weighted graphs, because \tilde{d} is large, β_1 is also large, so the above estimation formula does not apply.

For directed graphs, the above estimator does not apply.

Cora dataset [43], $n_l = 140, n = 2708$, when no self-loop is added, $\tilde{d} = 10858/2708 = 4.00$, $d_m = 168$, $d_{min} = 1$, $\beta_1 = -1$, the arithmetic mean of After adding the self-loop $\tilde{\lambda}_n = 1.4826$.

Citeseer dataset [43], $n_l = 120, n = 3327$, when no self-loop is added, $\tilde{d} = 2.7364$, $d_m = 99$, $d_{min} = 0$, after adding self-loop $\tilde{\lambda}_n = 1.5022$. In the Citeseer dataset, when the self-loop is not added, the degree of dozens of points is 0, which affects the estimation result.

Pubmed dataset [43], $n_l = 60, n = 19717$, when no self-loop is added, $\tilde{d} = 4.4960$, $d_m = 171$, $d_{min} = 1$, the arithmetic mean of After adding the self-loop $\tilde{\lambda}_n = 1.650$. □

Remark of Theorem 8. From the perspective of GCN, Y is also a graph signal, and the filter corresponding to the label propagation algorithm is an auto-regressive filter

$p_{ar}(\lambda) = 1/(1 + \alpha\lambda)$. The features of nodes on the graph can be regarded as a generalized label, which puts the label propagation algorithm and GCN under a unified framework.

Proof. GCN can be written as

$$H^{(l+1)} = \sigma(\tilde{D}^{-\frac{1}{2}} \tilde{A} \tilde{D}^{-\frac{1}{2}} H^{(l)} W^{(l)}) \quad (168)$$

where $\tilde{A} = A + I$. Matrix $\tilde{D}^{-1/2} \tilde{A} \tilde{D}^{-1/2} = I - \tilde{D}^{-1/2} \tilde{L} \tilde{D}^{-1/2}$ corresponds to the renormalization filter (renormalization filter, RNM filter) $p_{rnm}(\lambda) = (1 - \lambda)^k$. Two kinds of graph neural networks can be designed for this purpose, namely generalized label propagation. Note that the re-regularization technique is not used here, but is obtained directly from (48).

$$H^{(l+1)} = \sigma((I + \alpha D^{-1/2} L D^{-1/2})^{-1} H^{(l)} W^{(l)}) \quad (169)$$

and, enhanced graph convolution networks

$$H^{(l+k)} = \sigma((I - \tilde{D}^{-1/2} \tilde{L} \tilde{D}^{-1/2})^k H^{(l)} W^{(l)}) \quad (170)$$

It is equivalent to simplify graph convolution (SGC) [56].

Before inputting the feature X into the graph neural network, first use AR or RNM filter to filter it to obtain the filtered feature \bar{X} , and then set $H^{(0)} = \bar{X}$.

$$\bar{X}_{ar} = (I + \alpha D^{-1/2} L D^{-1/2})^{-1} X \quad (171)$$

$$\bar{X}_{rnm} = (I - \tilde{D}^{-1/2} \tilde{L} \tilde{D}^{-1/2})^k X \quad (172)$$

When the matrix L is large, in order to avoid the computational complexity caused by the direct inversion of $(I + \alpha D^{-1/2} L D^{-1/2})$ too high, by

$$(I + \alpha D^{-1/2} L D^{-1/2})^{-1} = \frac{1}{1 + \alpha} \sum_{i=0}^{+\infty} \left(\frac{\alpha}{1 + \alpha} D^{-1/2} A D^{-1/2} \right)^i \quad (173)$$

So take iterative

$$X^{(0)} = O, \dots, X^{(i+1)} = X + \frac{\alpha}{1 + \alpha} D^{-1/2} A D^{-1/2} X^{(i)} \quad (174)$$

then make

$$\bar{X}_{ar} = \frac{1}{1 + \alpha} X^{(t)} \quad (175)$$

When $t = [4\alpha]$, a better estimate can be obtained. \square

Proof of Theorem 13

Proof.

$$t_{k+1} = \frac{1 + \sqrt{4t_k^2 + 1}}{2} > \frac{1 + 2t_k}{2} = t_k + \frac{1}{2} \quad (176)$$

Take $t_0 = 1$ then $t_k > 1 + k/2 = (2 + k)/2$. \square

Proof of Theorem 17

Proof. For node i

$$\begin{aligned} \min_{w_i} & \frac{1}{2} w_i^T G^i w_i \\ \text{s.t.} & e^T w_i = 1 \end{aligned} \quad (177)$$

Lagrangian multiplier

$$L^i = \frac{1}{2} w_i^T G^i w_i - \lambda_i (e^T w_i - 1) = 0 \quad (178)$$

Through KKT condition

$$\nabla_{w_i} L^i = G^i w_i - \lambda_i e = 0, \nabla_{\lambda_i} L^i = e^T w_i - 1 = 0 \quad (179)$$

Note $G^{-1} = (G^i)^{-1}$

$$w_i = G^{-1} \begin{pmatrix} \lambda_i \\ \vdots \\ \lambda_i \end{pmatrix}, w_{ij} = \lambda_i \sum_{k \in N(i)} G_{jk}^{-1} \quad (180)$$

and $\sum_j w_{ij} = 1$, so

$$w_{ij} \leftarrow \frac{\lambda_i \sum_{k \in N(i)} G_{jk}^{-1}}{\sum_{j \in N(i)} (\lambda_i \sum_{k \in N(i)} G_{jk}^{-1})} = \frac{\sum_{k \in N(i)} G_{jk}^{-1}}{\sum_{l, s \in N(i)} G_{ls}^{-1}} \quad (181)$$

\square

Remark of Theorem 17. There is an iterative algorithm based on non-negative matrix factorization for solving this quadratic programming problem [64].

Proof. Eq. (113) is equivalent to

$$\begin{aligned} \min_W & \frac{1}{2} \|X - (C \odot W)X\|_F^2 + \frac{\mu}{2} \sum_{i=1}^m \|(C \odot W)\|_F^2 \\ \text{s.t.} & (C \odot W)e = e, W \geq 0 \end{aligned} \quad (182)$$

where $C_{ij} = \begin{cases} 1 & x_j \in N(x_i) \\ 0 & \text{otherwise} \end{cases}$, \odot denotes Hadamard product and $e = [1, 1, \dots, 1]^T$. Lagrangian multiplier

$$L = \frac{1}{2} \|X - (C \odot W)X\|_F^2 + \frac{\mu}{2} \|(C \odot W)e\|_F^2 - L^P \quad (183)$$

$$L^P = \lambda^T ((C \odot W)e - e) - \text{trace}(\Phi^T W) \quad (184)$$

$$\nabla_W L = C \odot ((C \odot W)X X^T + \mu(C \odot W)ee^T - X X^T - \lambda e^T) - \Phi \quad (185)$$

By KKT condition $\Phi_{ij} W_{ij} = 0, \nabla_W L = 0$ so

$$C_{ij} ((C \odot W)X X^T + \mu(C \odot W)ee^T - X X^T - \lambda e^T)_{ij} W_{ij} = 0 \quad (186)$$

Hence

$$W_{ij} = \begin{cases} W_{ij} \frac{(X X^T + \lambda e^T)_{ij}}{((C \odot W)X X^T + \mu(C \odot W)ee^T)_{ij}} & i \neq j \\ 0 & i = j \end{cases} \quad (187)$$

or $W_{ij} = 0$ when $x_j \notin N(x_i)$. For node i ,

$$\begin{aligned} \min_{w_i} & \frac{1}{2} w_i^T G^i w_i + \frac{\mu}{2} \|w_i\|_1^2 \\ \text{s.t.} & e^T w_i = 1, w_i \geq 0 \end{aligned} \quad (188)$$

Lagrangian multiplier

$$L^i = \frac{1}{2} w_i^T G^i w_i + \frac{\mu}{2} \|w_i\|_1^2 - \lambda_i (e^T w_i - 1) - \eta^T w_i \quad (189)$$

KKT condition

$$\begin{aligned} \nabla_{w_i} L^i &= G^i w_i + \mu e e^T w_i - \lambda_i e - \eta = 0 \\ \nabla_{\lambda_i} L^i &= e^T w_i - 1 = 0 \\ \eta &\geq 0, w_i \geq 0, \eta_j w_{j,i} = 0 \end{aligned} \quad (190)$$

so

$$w_i^T \nabla_{w_i} L^i = w_i^T G^i w_i + \mu (w_i^T e)^2 - \lambda_i w_i^T e = 0 \quad (191)$$

so

$$\lambda_i = (w_i^T G^i w_i + \mu(e^T w_i)^2)/e^T w_i \quad (192)$$

By $w_i^T G^i w_i \approx 0, e^T w_i - 1 = 0$

$$\lambda_i \approx \mu \Rightarrow \lambda = \mu e \quad (193)$$

So

$$w_{ij} \leftarrow w_{ij} \odot \frac{\mu}{(G^i w_i + \mu e e^T w_i)_j} \quad (194)$$

□

Proof of Theorem 18

Proof. First-order increment

$$\dot{x}_{ij} = x_i / \sqrt{\sum_i w_{ji}} - x_j / \sqrt{\sum_j w_{ij}} = x_i - x_j \quad (195)$$

If e is an all-one vector, then Q satisfies $Qe = 0$, and because $\sum_j w_{ij} = 1$, it can be assumed that $d_{ij} \sim N(0, 1/w_{ij})$, where w_{ij} represents the edge weights, assuming that the increments are independent, the joint probability distribution of x

$$\begin{aligned} p(x) &\propto \prod_{(i,j) \in E} p(\dot{x}_{ij}) \\ &\propto \prod_{(i,j) \in E} \exp(-\frac{1}{2} w_{ij} (x_i - x_j)^2) \\ &= \exp(-\frac{1}{2} \sum_{(i,j) \in E} w_{ij} (x_i - x_j)^2) \\ &= \exp(-\frac{1}{2} x^T L x) \end{aligned} \quad (196)$$

□

Proof of Theorem 19

Proof. For a graph with n nodes, we introduce n hyperedge nodes, and the hyperedge node e_i contains all nodes v_i and v_i 's neighborhood set $N(i)$ node. The labels of the hypernodes are weighted and summed by the node labels in $N(i)$, that is, $\sum_{j \in N_i} w_{ij} y_j$, so for the second order, the increment is defined as the difference between the hypernode and its corresponding node

$$\ddot{x}_i = x_i - \sum_{j \in N_i} w_{ij} x_j \quad (197)$$

where $\sum_{j \in N_i} w_{ij} = 1$. For the precision matrix $Q^h = \text{diag}\{\ddot{x}_i\}$ of the hypergraph, there is still $Q^h e = 0$, and e is an all-one vector, so it can be assumed that $d_i \sim N(0, 1)$, then

$$\begin{aligned} p(y) &\propto \prod_i p(\ddot{x}_i) \\ &\propto \exp(-\frac{1}{2} \sum_i (\sum_{j \in N_i} (w_{ij} x_j - x_i)^2)) \\ &= \exp(-\frac{1}{2} x^T (I - W)^T (I - W) x) \\ &= \exp(-\frac{1}{2} x^T L^T L x) \end{aligned} \quad (198)$$

□

Proof of Theorem 20

Proof. Consider the joint distribution of state x and observation y

$$\begin{aligned} Q^{-1} &= \begin{bmatrix} Q_{xx} & Q_{xy} \\ Q_{yx} & Q_{yy} \end{bmatrix}^{-1} \\ &= \begin{bmatrix} C_1^{-1} & -Q_{xx}^{-1} Q_{xy} C_2^{-1} \\ -C_2^{-1} Q_{yx} Q_{xx}^{-1} & C_2^{-1} \end{bmatrix} \\ &= \Sigma = \begin{bmatrix} \Sigma_{xx} & \Sigma_{xy} \\ \Sigma_{yx} & \Sigma_{yy} \end{bmatrix} \end{aligned} \quad (199)$$

Σ denotes covariance matrix.

$$\begin{aligned} C_1 &= Q_{xx} - Q_{xy} Q_{yy}^{-1} Q_{yx} \\ C_2 &= Q_{yy} - Q_{yx} Q_{xx}^{-1} Q_{xy} \end{aligned} \quad (200)$$

When

$$\begin{pmatrix} x \\ y \end{pmatrix} \sim N \left(\begin{pmatrix} \mu_x \\ \mu_y \end{pmatrix}, \begin{pmatrix} \Sigma_{xx} & \Sigma_{xy} \\ \Sigma_{yx} & \Sigma_{yy} \end{pmatrix} \right) \quad (201)$$

and

$$p(x|y) = \mathcal{N}(\mu_x + \Sigma_{xy} \Sigma_{yy}^{-1} (y - \mu_y), \Sigma_{xx} - \Sigma_{xy} \Sigma_{yy}^{-1} \Sigma_{yx}) \quad (202)$$

and $\mu_x = \mu_y = 0$, so

$$\mathbb{E}[x|y] = -Q_{xx}^{-1} Q_{xy} y \quad (203)$$

□

APPENDIX C SUPPLEMENTARY MATERIALS

A. Label propagation parameter selection in POGNN

Conduct the following experiments on the Cora dataset, setting hidden dim=16, learning rate=0.1, weight decay = 5e-4, epoch=50. The propagation process $H_{k+1} = AH_k \Theta_k$, Accuracy:

- $A = I - \eta L$, where
 - $\eta = 0.5$: 0.785
 - $\eta = 0.66$: 0.807. The distribution of the eigenvalues of the regularized Laplacian matrix of the Cora, citeseer and PubMed datasets after adding self-loops Histogram, in Cora, $\lambda_n \approx 1.5$, so take $\eta = 1/1.5 = 0.66$.
 - $\eta = 1$: 0.827. Equivalent to basic GCN.
 - $\eta = 2$: 0.449
- $A = (I + \eta L)^{-1}$, where
 - $\eta = 0.5$: 0.757
 - $\eta = 0.66$: 0.784
 - $\eta = 1$: 0.812
 - $\eta = 1.5$: 0.826
 - $\eta = 2$: 0.837
 - $\eta = 5$: 0.834

Convert the solution equation $Lf = 0$ into the solution differential equation $df/dt = -Lf, f_0 = y$ (similar to the heat conduction equation $du/dt = \Delta u$), then $f = e^{-Lt} y$. Given the eigenvalue decomposition $L = U \Lambda U^T$, then the heat kernel $e^{-Lt} = U e^{-\Lambda t} U^T$, which is consistent with the Fourier transform on the graph.

The process of iteratively solving $df/dt = -Lf$ with Euler's method is $f_{t+1} = (I - \eta L) f_t$, where $0 < \eta < 1$

TABLE X
TENTATIVE NETWORKS THAT COMBINE GCN AND LABEL PROPAGATION
VIA SUBSPACE LEARNING

Method	GCN	Net1	Net2	Net3
Acc	0.8130	0.8130	0.8210	0.8290

is the step size. When the activation function is not considered, the iterative process of the graph neural network is $H_{k+1} = (I - \eta L)H_k\Theta_k$, where Θ is the parameter of the neural network. When $\eta = 1$, the above formula is the general GCN iterative process $H_{k+1} = WH_k\Theta_k$, where W is the regularized adjacency matrix.

Compared the effect of taking different η values in the (0,1] interval, and set η as the reciprocal of the L spectral radius in its experiments, considering When adding the self-loop, $\eta = 1/\lambda_n$, we can use the previous guess to roughly estimate the value of η directly from the total number of edges and the total number of nodes. On the other hand, Because $\eta \in (0, 1]$, $I - \eta L = (1 - \eta)I + \eta A$, so this is also equivalent to introducing residual connection in GCN. And when the spectral radius of ηL is not greater than 1, the first-order Taylor expansion of $(I + \eta L)^{-1}$ is $I - \eta L$.

B. Tentative networks that combine GCN and label propagation via subspace learning

- 1) Net1 takes the result of GCN output as a low-dimensional representation of node features, and uses the [54] method to solve the weight matrix and perform the iterative process of label propagation.
- 2) Net2 takes the output of VGAE as a low-dimensional representation of node features, and uses the [54] method to solve the weight matrix and perform the iterative process of label propagation.
- 3) Net3 first trains a VGAE, the loss function = the classification error of VGAE + the error of VGAE decoding/reconstructing the original image + KL divergence, and the μ output by VGAE is used as a low-dimensional representation of node features, with [54] method solves the weight matrix and performs an iterative process of label propagation.

Using Adam optimization, learning rate=0.1, weight-decay=5e-4, dropout=0.5, hidden dim=16, and 100 iterations, the results are shown in table X, indicating that this method is superior to existing methods. LP in the table represents the label propagation algorithm [65] using the re-regularized adjacency matrix as the weight matrix.

C. Indicators in stock prediction

In technical analysis, technical indicators are mathematically calculated based on historical stock price opening (opening, high, closing, low), trading volume, etc. to quantify the rising or falling trend of prices, the power comparison between buyers and sellers, and investor sentiment. Technical indicators are a fundamental part of technical analysis and are usually drawn in chart form.

MACD

MACD is composed of the dispersion value DIF and the average difference and similarities DEA. The indicator calculates two fast and slow exponential moving averages (EMA) respectively. The most commonly used short and long periods are 12 days and 26 days. Then calculate the difference DIF between them, and then perform an exponential moving average operation on the difference to obtain DEM. The most commonly used parameter is 9. After two exponential moving average operations, the indicator can filter out the noise signals that often appear in the moving average for order verification, and retain the advantages of the moving average to a certain extent. The MACD histogram is the DIF minus twice the DEM. The mathematical expression is as follows:

$$DIF = EMA_{(close,12)} - EMA_{(close,26)}$$

$$DEM = EMA_{(DIF,9)}$$

$$MACD_{Histogram} = 2 \times (DIF - DEM)$$

RSI

RSI indicates the ratio of the sum of the price increase to the absolute sum of the overall increase and decrease within a certain time window, indicating the strength of the willingness to buy relative to the overall transaction, and the time window is generally 12. The mathematical expression is as follows:

$$RSI = 100 - \frac{100}{\left(1 + \frac{AverageGain}{AverageLoss}\right)}$$

KDJ

In the calculation of the Stochastic indicator, the highest price, lowest price and closing price in the calculation period are comprehensively considered, and the timing of the price trend reversal is predicted by comparing the closing price and the fluctuation range of the price. "Stochastic" refers to where the price is relative to its range over a period of time. First calculate RSV:

$$RSV = 100\% \times \frac{C_n - L_n}{H_n - L_n}$$

where C_n is the closing price on day n . H_n and L_n represent the highest and lowest prices in the past n days, respectively, and n is often 9. Then calculate K, D, J separately.

$$K_n = \alpha \times RSV_n + (1 - \alpha) \times K_{n-1}$$

$$D_n = \alpha \times K_n + (1 - \alpha) \times D_{n-1}$$

$$J_n = 3K_n - 2D_n$$

where $\alpha = 1/2$.

ROC

Rate of change (ROC) compares the stock price of the day with the stock price of a certain day before a certain number of days, indicating the size of its change speed, to reflect the degree of stock price change. ROC is essentially the change in the closing price within a day, and the commonly used parameter 12 is generally used. The mathematical expression is as follows:

$$ROC = 100\% \times \frac{C_i - C_{i-n}}{C_{i-n}}$$

where C_i is the closing price of the current day, and C_{i-n} is the closing price of n day before.

ATR

This indicator is a moving average of the True Range (TR), which represents the degree of volatility in this market. The length of the moving average window is generally 14, and the mathematical expression is as follows

$$TR = \max(H_i, C_{i-1}) - \min(L_i, C_{i-1})$$

$$ATR = SMA_{(TR,14)}$$

OBV

OBV digitizes the relationship between trading volume and stock price, two data representing stock market sentiment. Through the mutual change trend of the two, the driving force of the stock market is measured by the change in stock market trading volume, so as to judge the trend of stock price. If the closing price of a day is higher than the closing price of the previous trading day, then the OBV value for that day is equal to the OBV value of the last trading day plus the trading volume for that day. Otherwise, if the day's close is lower than the previous day's close, then today's OBV value is equal to the last day's OBV value minus that day's volume. The mathematical expression is as follows:

$$OBV = \begin{cases} OBV_{i-1} + V_i, & C_i \geq C_{i-1} \\ OBV_{i-1} - V_i, & C_i < C_{i-1} \end{cases}$$

REFERENCES

- [1] D. Bahdanau, K. Cho, and Y. Bengio, "Neural machine translation by jointly learning to align and translate," in *ICLR*, 2015.
- [2] T. Barfoot, *State estimation for robotics*. Cambridge University Press, 2017.
- [3] A. Beck and M. Teboulle, "A fast iterative shrinkage-thresholding algorithm for linear inverse problems," *SIAM Journal on Imaging Sciences*, vol. 2, no. 1, pp. 183–202, 2009.
- [4] M. Belkin and P. Niyogi, "Laplacian eigenmaps and spectral techniques for embedding and clustering," *Advances in Neural Information Processing Systems*, vol. 14, no. 6, pp. 585–591, 2001.
- [5] M. Belkin, P. Niyogi, and V. Sindhwani, "Manifold regularization: A geometric framework for learning from labeled and unlabeled examples," *Journal of Machine Learning Research*, vol. 7, no. 1, pp. 2399–2434, 2006.
- [6] K. M. Borgwardt, O. C. Soon, S. Stefan, S. Vishwanathan, A. J. Smola, and K. Hans-Peter, "Protein function prediction via graph kernels," *Bioinformatics*, vol. 21, no. suppl 1, pp. i47–i56, 2005.
- [7] S. Boyd, N. Parikh, E. Chu, B. Peleato, and J. Eckstein, "Distributed optimization and statistical learning via the alternating direction method of multipliers," *Foundations and Trends in Machine Learning*, vol. 3, no. 1, pp. 1–122, 2010.
- [8] J.-F. Cai, E. J. Candes, and Z. Shen, "A singular value thresholding algorithm for matrix completion," *Siam Journal on Optimization*, vol. 20, no. 4, pp. 1956–1982, 2010.
- [9] E. J. Candes, X. Li, Y. Ma, and J. Wright, "Robust principal component analysis?" *J. ACM*, vol. 58, no. 3, p. 11, 2011.
- [10] R. T. Q. Chen, Y. Rubanova, J. Bettencourt, and D. Duvenaud, "Neural ordinary differential equations," in *NeurIPS*, 2018.
- [11] I. Daubechies, M. Defrise, and C. Mol, "An iterative thresholding algorithm for linear inverse problems with a sparsity constraints," *Communications on Pure and Applied Mathematics*, vol. 57, no. 11, pp. 1413–1457, 2004.
- [12] A. P. Dempster, N. M. Laird, and D. B. Rubin, "Maximum likelihood from incomplete data via the em algorithm," *Journal of the Royal Statistical Society*, vol. 39, no. 1, pp. 1–38, 1977.
- [13] J. Devlin, M.-W. Chang, K. Lee, and K. Toutanova, "Bert: Pre-training of deep bidirectional transformers for language understanding," *CoRR*, 2018.
- [14] P. Dobson and A. Doig, "Distinguishing enzyme structures from non-enzymes without alignments," *Journal of molecular biology*, vol. 330, no. 4, pp. 771–783, 2003.
- [15] E. Elhamifar and R. Vidal, "Sparse subspace clustering," in *CVPR*, 2009.
- [16] H. Gao and S. Ji, "Graph u-nets," in *International Conference on Machine Learning*, 2019, pp. 2083–2092.
- [17] Z. Ghahramani and G. Hinton. (1996) Parameter estimation for linear dynamical systems. [Online]. Available: <http://mlg.eng.cam.ac.uk/zoubin/papers/tr-96-2.pdf>
- [18] J. Gilmer, S. S. Schoenholz, P. F. Riley, O. Vinyals, and G. E. Dahl, "Neural message passing for quantum chemistry," in *ICML*, 2017.
- [19] A. Graves, "Long short-term memory," *Neural Computation*, vol. 9, no. 8, pp. 1735–1780, 1997.
- [20] W. L. Hamilton, R. Ying, and J. Leskovec, "Inductive representation learning on large graphs," in *NeurIPS*, 2017.
- [21] C. Jin, J. Gao, Z. Shi, and H. Zhang, "Attcry: Attention-based neural network model for protein crystallization prediction," *Neurocomputing*, vol. 463, pp. 265–274, 2021.
- [22] C. Jin, Z. Shi, C. Kang, K. Lin, and H. Zhang, "Tlcrs: Transfer learning based method for protein crystallization prediction," *International Journal of Molecular Sciences*, vol. 23, p. 972, 1 2022.
- [23] C. Jin, Z. Shi, W. Li, and Y. Guo, "Bidirectional lstm-crf attention-based model for chinese word segmentation," *arXiv preprint arXiv:2105.09681*, 2021.
- [24] C. Jin, Z. Shi, K. Lin, and H. Zhang, "Predicting mirna-disease association based on neural inductive matrix completion with graph autoencoders and self-attention mechanism," *Biomolecules*, vol. 12, no. 1, p. 64, 2022.
- [25] C. Jin, Z. Shi, H. Zhang, and Y. Yin, "Predicting lncrna-protein interactions based on graph autoencoders and collaborative training," in *IEEE International Conference on Bioinformatics and Biomedicine (BIBM)*, Houston, USA, 9-12 December, 2021.
- [26] R. E. Kalman, "A new approach to linear filtering and prediction problems," *Journal of Fluids Engineering*, vol. 82, no. 1, pp. 35–44, 1960.
- [27] D. P. Kingma and J. Ba, "Adam: a method for stochastic optimization," in *3rd International Conference for Learning Representations (ICLR)*, 2015.
- [28] T. Kipf and M. Welling, "Semi-supervised classification with graph convolutional networks," in *ICLR*, 2017.
- [29] T. N. Kipf and M. Welling, "Variational graph auto-encoders," in *NeurIPS*, 2016.
- [30] J. Lee, I. Lee, and J. Kang, "Self-attention graph pooling," in *International Conference on Machine Learning*, 2019.
- [31] V. LEPETIT, N. F. MORENO, and P. FUA, "Epnnp: an accurate o (n) solution to the pnp problem," *International Journal of Computer Vision*, vol. 81, no. 2, pp. 155–166, 2009.
- [32] Q. Li, C. Long, T. Cheng, and W. E, "Maximum principle based algorithms for deep learning," *Journal of Machine Learning Research*, vol. 18, no. 1, 2017.
- [33] Q. Li, Z. Han, and X.-M. Wu, "Deeper insights into graph convolutional networks for semi-supervised learning," in *AAAI*, 2018.
- [34] Z. Lin, R. Liu, and Z. Su, "Linearized alternating direction method with adaptive penalty for low-rank representation," in *NeurIPS*, 2011.
- [35] G. Liu, Z. Lin, and Y. Yong, "Robust subspace segmentation by low-rank representation," in *International Conference on Machine Learning*, 2010.
- [36] Y. Ma, S. Wang, C. C. Aggarwal, and J. Tang, "Graph convolutional networks with eigenpooling," in *Proceedings of the 25th ACM SIGKDD International Conference on Knowledge Discovery & Data Mining*, 2019, p. 723–731.
- [37] A. Y. Ng, M. I. Jordan, and Y. Weiss, "On spectral clustering: Analysis and an algorithm," in *NeurIPS*, 2001.
- [38] L. Page, S. Brin, R. Motwani, and T. Winograd, "The pagerank citation ranking: Bringing order to the web," Stanford University, Tech. Rep., 1999.
- [39] B. Perozzi, R. Al-Rfou, and S. Skiena, "Deepwalk: Online learning of social representations," in *KDD*, 2014.
- [40] M. Qu, Y. Bengio, and J. Tang, "GMNN: Graph Markov neural networks," in *Proceedings of Machine Learning Research*, vol. 97, 2019, pp. 5241–5250.
- [41] H. E. Rauch, C. Striebel, and T. Tung, "Maximum likelihood estimates of linear dynamic systems," *AIAA Student Journal American Institute of Aeronautics and Astronautics*, vol. 3, no. 8, pp. 1445–1450, 1965.
- [42] F. Scarselli, M. Gori, A. C. Tsoi, M. Hagenbuchner, and G. Monfardini, "The graph neural network model," *IEEE Transactions on Neural Networks*, vol. 20, no. 1, pp. 61–80, 2009.

- [43] P. Sen, G. Namata, M. Bilgic, L. Getoor, B. Galligher, and T. E. Rad, "Collective classification of network data," *AI Magazine*, vol. 29, no. 3, p. 93, 2008.
- [44] N. Shervashidze, P. Schweitzer, E. Jan, V. Leeuwen, and K. M. Borgwardt, "Weisfeiler-lehman graph kernels," *Journal of Machine Learning Research*, vol. 12, no. 77, pp. 2539–2561, 2011.
- [45] J. Shi and J. Malik, "Normalized cuts and image segmentation," *IEEE Transactions on Pattern Analysis and Machine Intelligence*, vol. 22, no. 8, pp. 888–905, 2000.
- [46] Z. Shi, "Incorporating transformer and lstm to kalman filter with em algorithm for state estimation," *arXiv preprint arXiv:2105.00250*, 2021.
- [47] Z. Shi, H. Zhang, C. Jin, X. Quan, and Y. Yin, "A representation learning model based on variational inference and graph autoencoder for predicting lncrna-disease associations," *BMC Bioinformatics*, vol. 22, p. 136, 2021.
- [48] N. Srivastava, G. Hinton, A. Krizhevsky, I. Sutskever, and R. Salakhutdinov, "Dropout: a simple way to prevent neural networks from overfitting," *Journal of Machine Learning Research*, vol. 15, no. 1, pp. 1929–1958, 2014.
- [49] I. Sutskever, O. Vinyals, and Q. V. Le, "Sequence to sequence learning with neural networks," in *NeurIPS*, 2014.
- [50] K. K. Thekumparampil, C. Wang, S. Oh, and L.-J. Li, "Attention-based graph neural network for semi-supervised learning," *arXiv preprint arXiv:1803.03735*, 2018.
- [51] K.-C. Toh and S. Yun, "An accelerated proximal gradient algorithm for nuclear norm regularized least squares problems," *Pacific Journal of Optimization*, vol. 6, no. 3, pp. 615–640, 2010.
- [52] A. Vaswani, N. Shazeer, N. Parmar, J. Uszkoreit, L. Jones, A. N. Gomez, L. Kaiser, and I. Polosukhin, "Attention is all you need," in *NeurIPS*, 2017.
- [53] P. Velickovic, G. Cucurull, A. Casanova, A. Romero, P. Lio, and Y. Bengio, "Graph attention networks," in *ICLR*, 2018.
- [54] F. Wang and C. Zhang, "Label propagation through linear neighborhoods," in *ICML*, 2006.
- [55] J. Wang, F. Wang, C. Zhang, H. C. Shen, and L. Quan, "Linear neighborhood propagation and its applications," *IEEE Transactions on Pattern Analysis and Machine Intelligence*, vol. 31, no. 9, pp. 1600–1615, 2009.
- [56] F. Wu, T. Zhang, A. H. de Souza, C. Fifty, T. Yu, and K. Q. Weinberger, "Simplifying graph convolutional networks," in *ICML*, 2019.
- [57] L.-P. A. C. Xhonneux, M. Qu, and J. Tang, "Continuous graph neural networks," in *ICML*, 2020.
- [58] Z. Xia, L. Y. Wu, X. Zhou, and S. T. C. Wong, "Semi-supervised drug-protein interaction prediction from heterogeneous biological spaces," *Bmc Systems Biology*, vol. 4, no. Suppl 2, p. S6, 2010.
- [59] K. Xu, W. Hu, J. Leskovec, and S. Jegelka, "How powerful are graph neural networks?" in *International Conference on Learning Representations*, 2019.
- [60] K. Xu, J. Li, M. Zhang, S. S. Du, K.-i. Kawarabayashi, and S. Jegelka, "What can neural networks reason about?" in *ICLR*, 2020.
- [61] L. Yao, C. Mao, and Y. Luo, "Graph convolutional networks for text classification," *Proceedings of the AAAI Conference on Artificial Intelligence*, vol. 33, pp. 7370–7377, 2019.
- [62] R. Ying, J. You, C. Morris, X. Ren, W. Hamilton, and J. Leskovec, "Hierarchical graph representation learning with differentiable pooling," in *NeurIPS*, 2018.
- [63] G. Zhang, "Time series forecasting using a hybrid arima and neural network model," *Neurocomputing*, vol. 50, pp. 159–175, 2003.
- [64] W. Zhang, G. Tang, S. Wang, Y. Chen, S. Zhou, and X. Li, "Sequence-derived linear neighborhood propagation method for predicting lncrna-mirna interactions," in *BIBM*, 2018, pp. 50–55.
- [65] D. Zhou, O. Bousquet, T. N. Lal, J. Weston, and B. Scholkopf, "Learning with local and global consistency," *Advances in neural information processing systems*, vol. 16, no. 3, 2004.
- [66] X. Zhu, J. Lafferty, and Z. Ghahramani, "Semi-supervised learning using gaussian fields and harmonic functions," in *ICML*, 2003, pp. 912–919.
- [67] L. Zhuang, Z. Zhou, S. Gao, J. Yin, Z. Lin, and Y. Ma, "Label information guided graph construction for semi-supervised learning," *IEEE Transactions on Image Processing*, vol. 26, no. 9, pp. 4182–4190, 2017.